https://doi.org/10.5194/egusphere-2026-4112
Preprint. Discussion started: 21 July 2026

Modeling mineral dust aerosols in the Arctic with the regional model WRF-Chem 4.6.1

Louis Marelle[1], Rémy Lapere[1], Anderson Da Silva[1], Lucas Bastien[2], Ruth Price[2], and Jennie L. Thomas[2]

[1]LATMOS/IPSL, Sorbonne Université, UVSQ, CNRS, Paris, France
[2]Univ. Grenoble Alpes, CNRS, INRAE, IRD, Grenoble INP, IGE, 38000 Grenoble, France

Correspondence: Louis Marelle (louis.marelle@latmos.ipsl.fr)

Abstract. Important sources of mineral dust aerosols in the high latitudes, especially in the Arctic, are neglected in most atmospheric models. Here, we create a new description of mineral dust aerosol emissions including high-latitude dust sources, and implement it in a polar version of the WRF-Chem 4.6.1 model. We also improve the representation of mineral dust aerosol deposition processes. A 1-year-long quasi-hemispheric simulation for 2012 is evaluated against observations of surface concentrations and deposition fluxes at the Arctic surface. The updated model predicts 34 $\mathrm{Tg\,yr^{-1}}$ of emissions north of 60°N, and our evaluation shows dramatic improvements in model performance compared to the base model, to a state-of-the-art climate model, and to the CAMS reanalysis. We find that high latitude dust sources have significant impacts on several climate-relevant metrics in the Arctic, such as aerosol optical depth, ice nucleating particle concentrations, and especially mineral dust aerosol deposition to snow and ice, where high latitude sources are the main contributor over the Arctic sea ice pack. These results demonstrate the importance of taking high latitude dust emissions into account, provide a description of these sources reusable in other models, and open the way for future work to better estimate the climate impacts of high latitude dust sources.

1 Introduction

Mineral dust dominates the global atmospheric aerosol mass budget, with annual emissions ranging between 1500 and 5000 $\mathrm{Tg\,yr^{-1}}$ (Kok et al., 2021; Zhao et al., 2022). Mineral dust aerosols are primarily produced by the wind-driven erosion of soils in arid and semi-arid regions, although anthropogenic activities can influence dust emissions both directly and indirectly. Mineral dust aerosols have wide-ranging impacts on climate (Kok et al., 2023, 2026) through their direct interaction with radiation (aerosol-radiation interactions or ARI), their influence on cloud formation, especially primary cloud ice formation (aerosol-cloud interactions or ACI), and their deposition onto snow and ice and the resulting effect on surface albedo. In addition, mineral dust aerosols influence atmospheric chemistry and, following deposition to the surface, provide an important source of nutrients, including iron and phosphorus, to marine and terrestrial ecosystems (e.g., Jickells et al., 2005; Okin et al., 2004). Despite their importance, modeling mineral dust aerosols and quantifying their impacts remain a challenge, and global dust emissions still vary by a factor of five among the latest climate models of the Coupled Model Intercomparison Project (CMIP6, Zhao et al., 2022). These challenges are particularly evident at high latitudes, where CMIP6 models predict little or no dust

https://doi.org/10.5194/egusphere-2026-4112
Preprint. Discussion started: 21 July 2026

emissions (Zhao et al., 2022) despite evidence that high-latitude dust sources and their impacts can be significant (Meinander et al., 2022, 2025).

Polar climates might be particularly sensitive to locally sourced dust. Mineral dust are excellent ice nucleating particles (INP) leading to the formation of cloud ice crystals, and polar regions could be especially sensitive to dust INP due to the high prevalence of ice and mixed-phase clouds (Mioche et al., 2015; Listowski et al., 2019). In addition, deposited mineral dust could have more important effects on surface albedo in the frozen polar regions. Recently, the growing recognition of the importance of high-latitude dust has motivated the development of dedicated representations of their emissions in several atmospheric models. They have been incorporated in the global chemical-transport models FLEXDUST (Groot Zwaaftink et al., 2016, 2017) and SILAM (Sofiev et al., 2015; Meinander et al., 2022), and the regional chemical-transport model DREAM-ICELAND (Cvetkovic et al., 2022; Meinander et al., 2022). However, these chemical-transport models were developed to predict atmospheric composition and not their coupled impacts on atmospheric dynamics and climate. To our knowledge, only CAM-ATRAS (Kawai et al., 2023) includes high latitude dust emissions in a coupled global climate model, and no coupled regional climate model able to be run at finer scales is yet able to reproduce these sources.

In this study, we present a new description of mineral dust aerosols and their high-latitude emissions, implemented within the polar version of the regional WRF-Chem model (referred to hereafter as WRF-Chem-Polar). We also evaluate model results and the impacts of high latitude dust in the Arctic region, which could be the most sensitive to high latitude sources (Meinander et al., 2022, 2025). WRF-Chem-Polar includes many Arctic-specific developments, and has been extensively evaluated in the Arctic region (see Sect. 2), making it an excellent tool to represent mineral dust aerosols in the Arctic and their regional impacts on atmospheric dynamics and radiative forcing.

The baseline WRF-Chem-Polar model version is presented in Section 2. In Section 3, we describe our new mineral dust aerosol emission model, including how high-latitude sources are taken into account. In Section 4, we explain how we modified the representation of aerosol wet scavenging and sedimentation in WRF-Chem-Polar to better represent the lifetime of dust aerosols in the atmosphere. In Section 5 we present the model configuration for our evaluation runs, and finally in Section 6 we evaluate the new version of the model, we compare it to results obtained using baseline mineral dust emissions, and we quantify the impacts of these new emissions on measures relevant for understanding the climate impacts of mineral dust aerosols in the Arctic.

2 WRF-Chem-Polar: WRF-Chem 4.6.1 with updates for polar regions

We include new developments for mineral dust aerosols into the WRF-Chem model (Weather Research and Forecasting model, including chemistry, Skamarock et al., 2019, Grell et al., 2005). WRF-Chem is a coupled regional numerical weather and atmospheric composition model, that can include the coupled feedbacks of atmospheric composition on atmospheric dynamics, and can be used to perform dynamical downscaling of climate model simulations.

We implement our changes into WRF-Chem-Polar, a fork of WRF-Chem (currently up to date with WRF-Chem version 4.6.1), with additional developments for polar regions. The model and its earlier versions have been extensively evaluated

https://doi.org/10.5194/egusphere-2026-4112
Preprint. Discussion started: 21 July 2026

for their representation of local Arctic anthropogenic pollution (Marelle et al., 2016; Tuccella et al., 2017; Raut et al., 2022; Ioannidis et al., 2025), long-range transport of pollution from the midlatitudes and the seasonal cycle of Arctic pollution (Marelle et al., 2015, 2017; Raut et al., 2017; Whaley et al., 2022), natural aerosols and trace gases originating from the Arctic Ocean (Marelle et al., 2021; Ahmed et al., 2023; Ioannidis et al., 2023; Lapere et al., 2024a, 2026), deposition of aerosols onto snow (Thomas et al., 2017), atmospheric boundary layers over snow (Maillard et al., 2024), and the representation of clouds and radiation in the Arctic (Marelle et al., 2025; Lapere et al., 2026; Le Gars et al., 2026).

WRF-Chem-Polar was originally developed to investigate the impacts of anthropogenic pollution in the Arctic (Marelle et al., 2017), with improved emissions, aerosol sedimentation, deposition, and gas phase photolysis. Later changes focused on the representation of polar clouds, the radiative budget, and natural emissions of aerosols and trace gases, including: polar bromine and chlorine emissions and chemistry over sea ice (Marelle et al., 2021); atmospheric mercury (Ahmed et al., 2023); improved sea spray aerosol emissions from open water, including marine organics (Ioannidis et al., 2023; Lapere et al., 2024a); improved emissions from sea ice regions, including sea ice leads (Lapere et al., 2024a) and blowing snow (Marelle et al., 2021); new representations of aerosol-cloud interactions (Marelle et al., 2025), improved oceanic dimethylsulfide emissions and associated chemistry (Lapere et al., 2026), and many other smaller changes and bug fixes. Although WRF-Chem-Polar is developed with the aim of improving model performance in the polar regions, its development philosophy is to only include changes that can maintain or even improve model performance elsewhere, and not to overfit parameters and processes for the poles.

WRF-Chem-Polar model is continuously developed, and the latest released version before this study was Marelle et al. (2026d).

3 New mineral dust emissions in WRF-Chem-Polar

The default and most frequently used mineral dust emission model in WRF-Chem is based on the work of Ginoux et al. (2004) for the GOCART model, and is sometimes called the WRF-GOCART dust emission model. Here, we correct known shortcomings in the original WRF-GOCART formulation (following LeGrand et al., 2019), we update the model's dust source map to include potential polar emission sources, and we add new factors to represent the effect of soil moisture, snow cover and frozen soils that are important for emissions in the polar regions.

Besides WRF-GOCART, there are 2 advanced physically-based dust emission models in WRF-Chem, the Air Force Weather Agency (AFWA, LeGrand et al., 2019) and University of Cologne (UoC, Shao et al., 2011) models. We chose to base our developments on the older, more empirical model of Ginoux et al. (2004) because, first, it is simpler and less sensitive to input parameters that are poorly constrained in polar regions, and second, in a previous intercomparison of these schemes, LeGrand et al. (2019) showed that the original WRF-GOCART implementation, despite its flaws, was more skilled in reproducing the qualitative temporal and spatial variability of dust emissions at a large scale, (Figures 6 and 7 in LeGrand et al., 2019). We also hope that this relatively simple new emission model will be easier to implement in other models, including global climate models.

https://doi.org/10.5194/egusphere-2026-4112
Preprint. Discussion started: 21 July 2026

Our new developments are integrated in a new emission module in WRF-Chem, module_mineraldust_emis.F. The same emission module can be used to perform emissions to every aerosol model within WRF-Chem, in contrast to the usual WRF-Chem approach where emissions are calculated in each aerosol model code, in subroutines often reproduced with slight variations across the code base. New developments are controlled by the new WRF-Chem namelist option dust_erod_opt (to select the new dust source map presented in Sect. 3.1) and the preexisting option dust_opt (to select the new emission model presented in Sect. 3.3). The new option values are described in detail in the polar-options.md file documenting our changes at the root of the WRF-Chem-Polar model code. For now, the developments are compatible with GOCART aerosols, and with the 4-bin and 8-bin version of the MOSAIC aerosol model (Zaveri et al., 2008). Other aerosol models can easily be made compatible as long as their dust aerosol tracers have fixed aerosol diameter limits (Sect. 3.4).

3.1 Identifying mineral dust source regions at high latitudes

In the WRF-GOCART emission model, regions able to emit mineral dust aerosols are represented by the S-function (Ginoux et al., 2001), also sometimes called the erodibility, or the dust source function. It is meant to represent enhanced dust emissions from bare soils in topographical low points where alluvium accumulates, and it is calculated using the following empirical equation:

$$S = \begin{cases} \left(\dfrac{z - z_{min}}{z_{max} - z_{min}} \right)^5 & \text{if the soil is bare,} \\ 0 & \text{otherwise} \end{cases} \tag{1}$$

Where z is the local altitude of the ground surface (m), and z_{min} and z_{max} (m) are the minimum and maximum altitude in a $10° \times 10°$ surrounding region that broadly represents the scale of major hydrological basins.

The S-function originally included in the WRF-Chem model (Figure 1a,b) does not include any sources north of 52°N. It is not clear if this is due to missing information about bare soils at high northern latitudes at the time the S-function was created, or to intentional filtering of high latitude sources, either explicitly by a latitude cutoff or implicitly by only allowing emissions below some specific soil moisture or precipitation thresholds. Groot Zwaaftink et al. (2016) showed that regenerating the S-function from recent datasets revealed extensive potential dust sources in the Arctic.

We reproduce the work of Groot Zwaaftink et al. (2016) and regenerate the S-function from Eq. 1. We use the ETOPO 2022 global relief model for topography at 60 arc-second resolution (NOAA National Centers for Environmental Information, 2022) to determine z, z_{min}, and z_{max}, and the Global Land Cover by National Mapping Organizations version 3 (GLCNMOv3, Kobayashi et al., 2017) to identify bare and partially bare soil, using categories 10: “Sparse vegetation” and 17: “Bare area, unconsolidated (sand)”. We do not correct the S-function by the bare soil fraction in sparsely vegetated regions, because we choose to do it instead at model runtime using the time-varying bare soil fraction (Sect. 3.3), to allow for more accurate seasonal variations of the emissions.

https://doi.org/10.5194/egusphere-2026-4112
Preprint. Discussion started: 21 July 2026

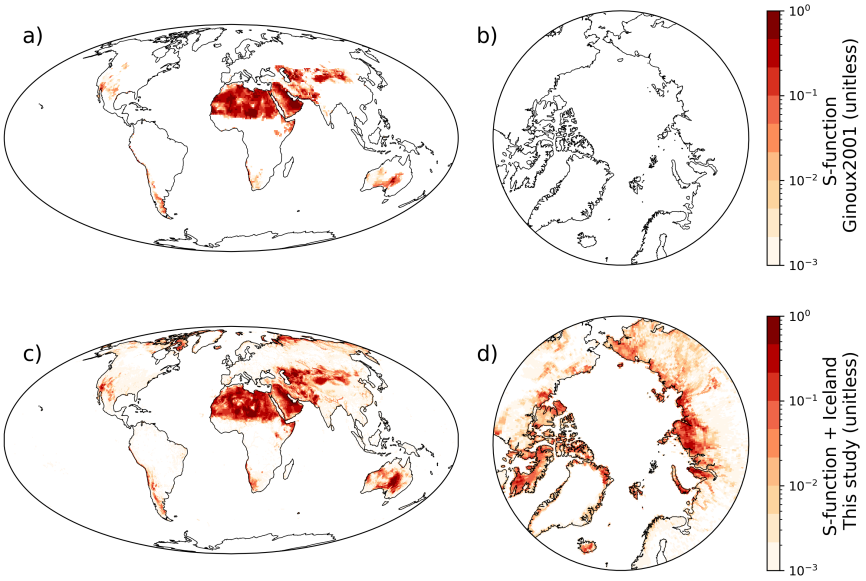

Figure 1. S-function, indicating potential mineral dust emission regions. (a-b) Original Ginoux et al. (2001) dataset used in WRF-Chem. (c-d) S-function recalculated in this study, and replaced by detailed soil erodibility data in Iceland.

As discussed in Groot Zwaaftink et al. (2016), the S-function cannot accurately reproduce potential emissions in Iceland, a major high latitude dust emission hotspot. There, we replace the calculated values of the S-function by the detailed erodibility map from Figure 2 of Cvetkovic et al. (2022).

The result of combining Eq. 1 and the Icelandic erodibility map of Cvetkovic et al. (2022) are shown on Figure 1c,d. It reveals potential high latitude dust emission hotspots in the Canadian Archipelago, Northern Siberia, Iceland and coastal Greenland. The S-function dataset is provided at 60s, 0.1° and 0.5° resolutions as NetCDF files in Marelle (2026b), also including the Python scripts used to generate it.

3.2 Threshold friction velocity for mineral dust aerosol emissions

In source regions, mineral dust emissions are initiated by the saltation bombardment of loose soil by large lofted particles, when the friction velocity U^* exceeds a threshold value for saltation. In our model, the threshold friction velocity is based on the classical formulation of Marticorena and Bergametti (1995), as in Ginoux et al. (2004), and depends on soil grain size and density:

$$U^*_{ts,p} = f_{fécan1999} \times 0.129 \times 10^{-2} \frac{\sqrt{\frac{\rho_p g D_p}{\rho_{air}} \left(1 + \frac{6 \times 10^{-7}}{\rho_p g D_p^{2.5}}\right)}}{\sqrt{1.928(1.7546 \times 10^6 D_p^{1.56} + 0.38)^{0.092} - 1}} \quad (2)$$

https://doi.org/10.5194/egusphere-2026-4112
Preprint. Discussion started: 21 July 2026

Table 1. Saltation particle size classes and their properties in the soil, from LeGrand et al. (2019). $clayfrac$, $siltfrac$ and $sandfrac$ are the soil clay, silt and sand fractions (unitless)

Saltation size class p	Effective soil diameter D_p (µm)	Soil class	Size class fraction $fracsize_p$ (unitless)	Particle density ρ_p ($\mathrm{kg\,m^{-3}}$)
1	1.42	Clay	$1\times clayfrac$	2500
2	2.74	Silt	$0.2\times siltfrac$	2650
3	5.26	Silt	$0.2\times siltfrac$	2650
4	10	Silt	$0.2\times siltfrac$	2650
5	19	Silt	$0.2\times siltfrac$	2650
6	36.2	Silt	$0.2\times siltfrac$	2650
7	69	Sand	$1/3\times sandfrac$	2650
8	131	Sand	$1/3\times sandfrac$	2650
9	250	Sand	$1/3\times sandfrac$	2650

Where all variables are in SI units: ρ_p is the soil grain density ($\mathrm{kg\,m^{-3}}$), D_p the soil grain diameter (m), g is the gravitational acceleration ($\mathrm{m\,s^{-2}}$), ρ_{air} is the air density ($\mathrm{kg\,m^{-3}}$). As discussed in LeGrand et al. (2019), the values of ρ_p and D_p from Ginoux et al. (2004) do not correctly represent soil properties. Following their recommendations, we use instead the values of ρ_p and D_p presented in Table 1, that depend on the clay, silt and sand fractions in the soil.

Compared to Ginoux et al. (2004), we include in Eq. 2 $f_{fécan1999}$ (unitless), an empirical scaling factor to increase the threshold velocity over wet soils in semi-arid regions (Fécan et al., 1999). It is a function of $smois_{grav}$, the gravimetric soil moisture ($\mathrm{kg\,kg^{-1}}$), and $smois_{thresh}$ the threshold soil moisture ($\mathrm{kg\,kg^{-1}}$):

$$f_{fécan1999} = \begin{cases} \sqrt{1. + 27.72(smois_{grav} - smois_{thresh})^{0.68}}, & \text{if } smois_{grav} > smois_{thresh}, \\ 1, & \text{otherwise} \end{cases} \quad (3)$$

The threshold soil moisture $smois_{thresh}$ is also from Fécan et al. (1999), and is a function of the soil clay fraction $clayfrac$ (unitless).

$$smois_{thresh} = 0.17 \times clayfrac + 0.14 \times clayfrac^2 \quad (4)$$

In eqs. 3 and 4, $smois$ and $clayfrac$ were converted to fractional units, instead of percentage values in Fécan et al. (1999).

3.3 Source function for mineral dust aerosol emissions

Once saltation occurs, the emission flux of mineral dust aerosol to the atmosphere F_{dust} ($\mathrm{\mu g\,m^{-2}\,s^{-1}}$) is calculated as the sum of the emission fluxes $F_{dust,p}$ for each saltation size class p, individually weighted by $fracsize_p$, the fraction of each size class in the soil.

https://doi.org/10.5194/egusphere-2026-4112
Preprint. Discussion started: 21 July 2026

$$F_{dust} = \sum_{p} (fracsize_p \times F_{dust,p}) \tag{5}$$

$fracsize_p$ depends on the fraction of clay, silt and sand in the model grid cell, and on the assumed granulometry of clay, silt and sand available for saltation, set using the parameters in Table 1. Since $clayfrac + siltfrac + sandfrac = 1$ and since the sum of the size class fractions within each soil class is also equal to 1, the sum of all $fracsize_p$ is also always equal to 1.

Finally, $F_{dust,p}$ ($\mu g\,m^{-2}\,s^{-1}$) is calculated using eq. 6, a modified form of the Ginoux et al. (2004) source function:

$$F_{dust,p} = CS(1 - greenfrac) f_{freeze} f_{moisture} U_{10m}^2 \left(U_{10m} - \frac{U_{10m} U_{ts,p}^*}{U^*} \right), \text{ if } U^* > U_{ts,p}^* \tag{6}$$

Where S is the Ginoux S-function from eq. 1 (unitless); $greenfrac$ is the grid cell vegetation fraction (unitless); f_{freeze} is the soil freezing and snow cover correction factor (unitless); $f_{moisture}$ is the soil moisture correction factor (unitless); U_{10m} is the 10-m wind speed ($m\,s^{-1}$), U^* is the friction velocity ($m\,s^{-1}$), and $U_{ts,p}^*$ is the threshold friction velocity ($m\,s^{-1}$). C is a dimensional scaling factor ($0.2\ \mu g\,m^2\,s^{-5}$), and its value is taken directly from the original implementation of the WRF-GOCART scheme (discussed in LeGrand et al., 2019), and is not re-adjusted for this study.

Compared to Ginoux et al. (2004), we include the additional f_{freeze} and $f_{moisture}$ scaling factors for frozen soil and soil moisture, the time-varying bare soil fraction scaling $(1 - greenfrac)$, and we also scale the threshold velocity U_{ts}^* to convert it from a friction velocity to a 10-m velocity more appropriate for the formulation.

The soil moisture correction factor $f_{moisture}$ depends on the volumetric soil moisture $smois_{vol}$ ($m^3\,m^{-3}$) (UNCCD, 2022)

$$f_{moisture} = \begin{cases} 1, & \text{if } smois_{vol} \le 0.15\,m^3\,m^{-3}, \\ 0.15/smois_{vol}, & \text{if } smois_{vol} > 0.15\,m^3\,m^{-3} \end{cases} \tag{7}$$

The cutoff factor for soil freezing and snow cover f_{freeze} depends on the skin temperature T_{skin} (K), and on the snow height at the surface $snow_h$ (m). The critical snow height for cutting emissions is chosen at $0.1\ m$, consistently with the rest of the WRF-Chem model.

$$f_{freeze} = \begin{cases} 0, & \text{if } T_{skin} \le T_{freeze} \text{ or } snow_h > 0.1\,m, \\ 1, & \text{if } T_{skin} > T_{freeze} \end{cases} \tag{8}$$

Where the soil freezing temperature T_{freeze} (K) is a function of the volumetric soil moisture $smois_{vol}$ ($m^3\,m^{-3}$) (UNCCD, 2022)

$$T_{freeze} = \begin{cases} 260\,K, & \text{if } smois_{vol} < 0.2, \\ 260 + 12\dfrac{(smois_{vol} - 0.2)}{0.2}, & \text{if } 0.2 \le smois_{vol} < 0.4, \\ 272\,K & \text{if } 0.4 \le smois_{vol} \end{cases} \tag{9}$$

https://doi.org/10.5194/egusphere-2026-4112
Preprint. Discussion started: 21 July 2026

3.4 Size distribution of emitted mineral dust aerosols

The total aerosol emission flux to the atmosphere from Eq. 5, F_{dust}, is assumed be partitioned in size following the size distribution of Kok (2011).

$$\frac{dV_d}{dlnD_d} = \frac{D_d}{c_V}\left[1 + erf\left(\frac{ln(D_d/\bar{D}_s)}{\sqrt{2}ln\sigma_s}\right)\right] exp\left[-\left(\frac{Dd}{\lambda}\right)^3\right] \tag{10}$$

Where V_d is the aerosol volume (μm^3), D_d is the aerosol dry diameter (μm), $\sigma_s = 3.0$ is the geometric standard deviation of the distribution, $\bar{D}_s = 3.4\,\mu m$ is the median aerosol diameter of the distribution by volume, $c_V = 12.62\,\mu m$ is a normalization constant, $\lambda = 12.0\,\mu m$ is the dust aggregate side crack propagation length, and erf is the error function.

In the sectional aerosol models used within WRF-Chem-Polar (MOSAIC-4bin, MOSAIC-8bin, GOCART with 5 dust size bins) the diameter limits of the aerosol sections do not change during the simulation, and the size distributions at emissions can be precalculated. We integrate Eq. 10 over these size section limits to obtain fixed volume scaling factors used to distribute the total mass flux calculated in Eq. 6 to the bins of each aerosol model. The Python code used to perform this integration is available at Marelle et al. (2026a).

When this integration is performed over the MOSAIC aerosol size bins in WRF-Chem, 27.2 % of the total aerosol mass is emitted above the maximum aerosol diameter of 10 µm. For GOCART aerosols, the maximum diameter is larger at 20 µm, and the missing mass is only 0.25 %. We choose to discard this part of the emission flux outside of the aerosol size range, to avoid assigning it to a smaller size and thus overestimating its lifetime in the atmosphere. We think that this is reasonable, if we assume that these large particles get deposited to the surface relatively quickly (approximately $2\,cm\,s^{-1}$ at a 20 µm diameter). However, in some conditions, coarse dust aerosols can be transported over long distances, and modelers might prefer to include this missing mass at the risk of overestimating its lifetime. We added an option in the code (off by default) to emit it to the coarser size bin if wanted.

3.5 New land mask and land surface classification in WRF-Chem-Polar

Arctic mineral dust sources are strong in coastal areas, but we found an issue in the WRF and WRF-Chem models where coastal land is often incorrectly classified as water, preventing emissions (Figure 2a). This is due to errors in the land cover dataset and in how it is used in the WRF preprocessing system (WPS) part of the code, at the "geogrid" step that defines the model grid and interpolates static geographical data onto it.

This issue is partly caused by the procedure for setting the land surface classification in geogrid. First, for each model grid cell, the nearest point in the static land use dataset is selected. The default dataset is a modified 21-category land use classification mosaic based on the MODIS land cover type. Second, the dominant category in the grid cell is selected, and if it is a land category, the grid cell is categorized as land, otherwise it is categorized as water. Since there are 19 land categories but only 2 water categories (water and lakes) in this classification, in coastal areas the dominant category is much more likely to be water, even if it represents less than 50% of the grid cell area.

https://doi.org/10.5194/egusphere-2026-4112
Preprint. Discussion started: 21 July 2026

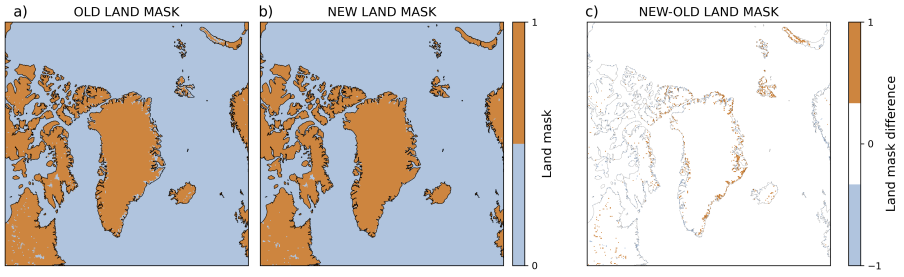

Figure 2. Example WRF model land mask at a 25 km horizontal resolution. a) Original mask, showing spurious open water points, most notably around Greenland, Iceland, Svalbard, and Novaya Zemlya. b) New mask calculated from MODIS MCD12Q1.061 land cover data, correcting these issues. c) difference, showing new land in brown and new water in light blue.

We also found a separate issue in the land cover classification dataset, where high latitude glaciers and ice caps are often incorrectly categorized as lakes. The origin of the lake data in the WRF land use is not documented, so it is not clear what caused this issue in the original lake dataset.

Last but not least, it is also not clear what time period was used to generate WRF land cover categories, but since this dataset has not been modified recently, it is likely not up to date with the rapidly evolving distribution of glaciers and vegetation in the Arctic.

In order to fix these issues, we regenerate the modified 21 category MODIS land use in WRF from the original MODIS 17-category dataset. Specifically, we use the MODIS/Terra+Aqua Land Cover Type Yearly L3 Global product at 0.05° resolution, version 6.1 (MCD12C1.061, Friedl and Sulla-Menashe, 2022). Furthermore, instead of using a sub-grid land cover mosaic in each pixel, only the dominant category in MCD12C1.061 is kept, to avoid the weighting issue presented above. This is unlikely to degrade model results because almost every common configuration of WRF and WRF-Chem and every past configuration of WRF-Chem-Polar only represents the surface by its dominant classification type.

Category 21 (lakes) in the new dataset is assigned by identifying MODIS water points contained in any of the Natural Earth Data lake shapefiles (Kelso and Patterson, 2010). We do not re-generate WRF categories 18, 19, and 20 corresponding to tundra, because the procedure to create them was not documented, and because we find that extended areas defined as grassland in MODIS are defined as mixed tundra (woodland+grassland) in WRF, which warrants further review of these data.

We generate this new WRF landuse dataset for the full MCD12C1.061 time span (years 2003-2024), and the dataset for the closest year to the simulation start date is selected at runtime. Following the WRF nomenclature, the dataset is named modis_landuse_20class_3m_with_lakes. We show on Figure 2b how using the new dataset leads to a more realistic WRF land mask in the Arctic.

The full dataset and the Python scripts to generate it are provided at Marelle (2026a). We generated the landuse dataset using the highest MCD12Q1.061 resolution available as a global single raster. This resolution is relatively coarse, at 0.05° (approximately 5.5 km in latitude), and for this reason we do not recommend using it with high resolution WRF runs (e.g., $< 10\ km$). For high resolution applications, the dataset could be regenerated in the future at full MODIS resolutions (~500 m).

https://doi.org/10.5194/egusphere-2026-4112
Preprint. Discussion started: 21 July 2026

4 Additional developments for simulating mineral dust aerosols in WRF-Chem-Polar

Studies focused on mineral dust aerosols using the WRF-Chem model (e.g., LeGrand et al., 2019; Ukhov et al., 2021; Drakaki et al., 2022; Pino-Carmona et al., 2024) usually select a simplified aerosol setup based on the GOCART model (Chin et al., 2002; Ginoux et al., 2004), which does not include gas-phase chemistry or the production of secondary aerosols. In GOCART, dust aerosols are represented by 5 size-sectional dust tracers only affected by emissions, advection, mixing, deposition, and sedimentation.

There is no wet scavenging by grid-scale clouds in GOCART within WRF-Chem. This is a serious limitation for reproducing the long-range transport of dust from lower latitudes to the poles, or the evolution of dust concentrations at high latitudes. In addition, the sedimentation of GOCART aerosols in WRF-Chem uses a simplified "upwind" numerical scheme which is known to be very diffusive, and could further degrade the representation of the long-range aerosol transport (Drakaki et al., 2025). These shortcomings are corrected below.

4.1 New wet scavenging for GOCART mineral dust aerosols

The GOCART aerosol model in WRF-Chem does not include wet scavenging by grid-scale clouds. Here we included a simple aerosol wet scavenging module in WRF-Chem-Polar, module_aer_wetscav_simple.F, performing the calculations described below. It is enabled by the preexisting namelist option wetscav_onoff = 1.

4.1.1 Wet scavenging of GOCART mineral dust by rainout processes

Rainout (also sometimes called in-cloud wet scavenging) is the removal of aerosols activated in clouds by the conversion of cloud droplets and ice crystals to precipitation. In our simple model, rainout is only performed for aerosols activated within liquid cloud droplets, because ice nucleation is comparatively very inefficient except at temperatures where homogeneous freezing starts to dominate, near -38°C and below. In addition, we found that trying to model wet scavenging in mixed phase clouds using such simplified parameterizations (as in, e.g., Luo et al., 2020) strongly overestimates wet scavenging because dust aerosols activated in ice crystals end up being artificially removed by precipitation generated from the liquid phase.

The aerosol concentration removed by rainout $C_{rainout}$ ($\mu g\,kg^{-1}$) is calculated as:

$$C_{rainout} = qlsink \times \Delta t \times cloudbornefrac \times C_{aer} \tag{11}$$

Where C_{aer} is the aerosol concentration in the grid cell ($\mu g\,kg^{-1}$) , $qlsink$ is the rate of conversion of cloud water to precipitation calculated in the cloud microphysics model ($kg\,kg^{-1}\,s^{-1}$), Δt is the model time step (s), and $cloudbornefrac$ is the fraction of aerosols activated in clouds ($unitless$), calculated as follows:

$$cloudbornefrac = liquidfrac \times cloudfrac \times aeraqfrac \tag{12}$$

Where $cloudfrac$ is the cloud fraction in the grid cell ($unitless$), $liquidfrac$ is the fraction of total cloud water in the liquid phase, and $aeraqfrac$ is a parameter representing the activation efficiency of the species in cloud liquid droplets ($unitless$).

https://doi.org/10.5194/egusphere-2026-4112
Preprint. Discussion started: 21 July 2026

Table 2. A_i and B_i coefficients for the calculation of the washout loss rate, for each precipitation type and depending on the aerosol diameter, from Luo et al. (2020)

Class i	Name	A_i ($\mathrm{kg}^{-\mathrm{B_i}}\,\mathrm{m}^{2\mathrm{B_i}}\,\mathrm{s}^{\mathrm{B_i}-1}$)	B_i (unitless)
Fine aerosols, $D_d < 2\,\mu\mathrm{m}$			
1	rain	4.3×10^{-6}	0.61
2	snow	8.8×10^{-6}	0.96
3	ice	1.76×10^{-6}	0.96
Coarse aerosols, $D_d \geq 2\,\mu\mathrm{m}$			
1	rain	2.6×10^{-4}	0.79
2	snow	4.2×10^{-4}	0.96
3	ice	8.4×10^{-5}	0.96

We chose $aeraqfrac = 0.5$ for mineral dust aerosols, 1.0 for sea salt, and 0.8 for hydrophilic OC and BC, consistently with the values already present in the wet scavenging code of the Grell subgrid cumulus model in WRF-Chem.

4.1.2 Wet scavenging of GOCART mineral dust by washout processes

Washout (also sometimes called below-cloud wet scavenging or impaction scavenging) is the removal of aerosols or trace gases by impaction with precipitation. In our simple wet scavenging model, we represent these processes by the formulation of Luo et al. (2019) and Luo et al. (2020), where the concentration of aerosols removed by washout $C_{washout}$ is a function of the precipitation type (rain, snow, ice); the fraction of the model grid cell experiencing precipitation $frac_{washout}$, and whether the aerosol is coarse or fine.

$$C_{washout} = frac_{washout}(1 - e^{-washoutrate \times \Delta t})C_{aer} \tag{13}$$

Where $washoutrate$ (s^{-1}) is the sum of the washout loss rates from each precipitation type i (rain, snow, ice), calculated from RR_i, the precipitation rate for precipitation type i ($\mathrm{kg\,m^{-2}\,s^{-1}}$)

$$washoutrate = \sum_i A_i \left(\frac{RR_i}{frac_{washout}} \right)^{B_i} \tag{14}$$

Where empirical coefficients A_i (units $\mathrm{kg}^{-\mathrm{B_i}}\,\mathrm{m}^{2\mathrm{B_i}}\,\mathrm{s}^{\mathrm{B_i}-1}$) and B_i (unitless) are given in Table 2 and depend on the the precipitation type and whether the aerosol is coarse or fine. As a simplification, we use the aerosol dry diameter D_d instead of the wet diameter to determine this.

The fraction of the grid cell experiencing washout, $frac_{washout}$, represents the fraction of the grid cell where precipitation is present, and is taken as the maximum between the fraction of the grid cell experiencing rainout, $frac_{rainout}$, and of $frac_{washout}$ in the vertical level directly above it, such that it can only increase with decreasing altitude. $frac_{rainout}$ (unitless)

https://doi.org/10.5194/egusphere-2026-4112
Preprint. Discussion started: 21 July 2026

is calculated following Luo et al. (2019):

$$frac_{rainout} = \frac{rainrate}{\left(k_0 + \frac{rainrate}{cloudwater}\right) \times cloudwater} cloudfrac \quad (15)$$

Where $rainrate$ is the precipitation formation rate ($\mathrm{kg\,kg^{-1}\,s^{-1}}$), $k_0 = 10^{-4}\,\mathrm{s^{-1}}$ is a first-order rainout rate, and $cloudwater$ is the total condensed cloud water mixing ratio ($\mathrm{kg\,kg^{-1}}$). Compared to Luo et al. (2019), we added a scaling by the cloud fraction $cloudfrac$, because otherwise $frac_{rainout}$ can easily exceed $cloudfrac$ even though precipitation cannot be generated out of the cloud.

We do not include resuspension of scavenged aerosols by evaporating precipitation, because tests showed that this could lead to very high, unrealistic spikes in surface aerosol concentrations when precipitation evaporates, even when applying a strong scaling factor to the process (not shown, tested down to 0.1 in an earlier version of the model). It is possible that aerosols released by resuspension processes in the real atmosphere are still too large and sediment too fast to affect concentrations durably, because they are still hydrated or because they coagulate in the evaporating raindrop or snowflake.

4.2 New sedimentation for GOCART mineral dust aerosols

The GOCART aerosol model in WRF-Chem performs sedimentation with a simple first-order upwind advection scheme, which is known to cause severe numerical diffusion. We reimplement the sedimentation module to perform advection with the scheme of Després and Lagoutière (1999), a remarkably anti-diffusive approach, following the recommendations of Mailler et al. (2021).

The new module is called module_aer_settling_simple.F, and controlled by the new namelist option aer_settling_opt. The module is currently only enabled for the GOCART aerosol model, but we created it so that it can be used in the future to perform sedimentation for other aerosol models in WRF-Chem.

Sedimentation is performed with a first-order scheme similar to the typical upwind scheme, where the new concentration at vertical level k, $c(k)$ is calculated from the upwind concentrations c', the sedimentation velocity $vsettl$ ($\mathrm{m\,s^{-1}}$), the vertical level depth Δz (m) and the model timestep Δt (s)

$$c(k,t+1) = c(k,t) + c'(t) \times \frac{vsettl(k+1) \times \Delta t}{\Delta z(k+1)} \quad (16)$$

, taking the proper precautions of subsetting the time step if it is larger than what is allowed by the CFL condition, and converting the native WRF-Chem aerosol mixing ratios in $\mathrm{\mu g\,kg^{-1}}$ to vertically resolved loads in $\mathrm{\mu g\,m^{-2}}$ that can be transferred between vertical levels of different depths and air densities, before converting them back.

The difference between the approach of Després and Lagoutière (1999) and the usual upwind scheme is in the calculation of $c'(t)$, where instead of $c(k+1,t)$, the following formulation is used:

$$c' = c(k+1) + \frac{1-\nu}{2} \times Max(0, Min(\frac{2}{\nu} \times \frac{c(k+1)-c(k+2)}{c(k)-c(k+1)}, \frac{2}{1-\nu})) \times (c(k)-c(k+1)) \quad (17)$$

Where $\nu = vsettl \times \Delta t / \Delta z$ (unitless) is the Courant number.

https://doi.org/10.5194/egusphere-2026-4112
Preprint. Discussion started: 21 July 2026

As showed in Mailler et al. (2021), using the result of Eq. 17 in the first-order advection scheme of Eq. 16 almost completely cancels the effect of numerical diffusion in vertical advection, at a minimal computational cost.

5 WRF-Chem-Polar simulation setup

In order to evaluate the new dust emission model, we perform a 1-year simulation from 2012-01-01 to 2013-01-01, at $100\,\mathrm{km}\times100\,\mathrm{km}$ horizontal resolutions, on the quasi-hemispheric domain presented on Figure 3a. We use 70 vertical levels from the surface to $50\,\mathrm{hPa}$, with the lowest level top at $20\,\mathrm{m}$ AGL. Initial and boundary conditions for meteorology are from the ERA5 reanalysis (Copernicus Climate Change Service, 2017), with spectral nudging to ERA5 winds, geopotential, and temperature above the $700\,\mathrm{km}$ scale. Initial and boundary conditions for aerosols including mineral dust are from the CESM2.2 CAM-Chem model (Tilmes et al., 2022).

The detailed WRF-Chem simulation setup is given in the namelists and configuration files available at Marelle et al. (2026b). It follow best practices from previous simulations evaluating WRF-Chem-Polar. Briefly, we use the Noah Land Surface Model (Tewari et al., 2004), the MYNN 2.5 surface layer and boundary layer (Nakanishi and Niino, 2009), RRTMG for radiative tranfer (Iacono et al., 2008), Thompson 2-moment microphysics (Thompson et al., 2008), and Grell-3 cumuli (Grell and Dévényi, 2002) including tracer transport and removal by subgrid clouds. The cloud fraction used for radiative transfer and for wet scavenging by grid-scale clouds is diagnosed following Xu and Randall (1996).

To model mineral dust aerosols, we use the simple GOCART aerosol model already presented above (Ginoux et al., 2004, GOCART_SIMPLE in WRF-Chem), only representing primary black carbon (BC), organic carbon (OC), sea salt, sulfate, and mineral dust. In GOCART_SIMPLE, mineral dust is represented by 5 size bins, covering the dry diameter range from $200\,\mathrm{nm}$ to $20\,\mu\mathrm{m}$. We also use the new developments to the GOCART_SIMPLE aerosol model presented in Sect. 4.

Primary sea salt and marine organic emissions are included following Ioannidis et al. (2023) and Lapere et al. (2024a), and emissions from sea ice leads following Lapere et al. (2024a). Sea salt emissions from blowing snow over sea ice are also included (Marelle et al., 2021). Emissions of mineral dust use the new developments described in Sect. 3. We include anthropogenic and fire emissions of primary BC, OC and sulfate aerosols, and other unspeciated primary PM_{10} and $PM_{2.5}$, from the ECLIPSEv6 (Klimont et al., 2017) and FINNv2.5 (Wiedinmyer et al., 2023) inventories respectively. These emissions and sea salt emissions do not influence mineral dust directly, except through the effect of aerosol-radiation interactions on modeled meteorology.

We enable aerosol-radiation interactions (ARI) in order to diagnose the effect of our changes on modeled aerosol optical depth (AOD), and to better reproduce the observed meteorology, especially during summer when the AOD from fire aerosols can be significant. We do not enable aerosol-cloud interactions (ACI), because the GOCART_SIMPLE aerosol model in WRF-Chem does not represent secondary sulfate, which is critical to predict cloud condensation nuclei (CCN). For this reason, we use a version of the Thompson cloud microphysics scheme that is only double-moment for ice, but single-moment for liquid water (Thompson et al., 2008), with fixed droplet concentrations of $100\,\mathrm{cm}^{-3}$. Primary ice formation follows Bigg (1953) for

https://doi.org/10.5194/egusphere-2026-4112
Preprint. Discussion started: 21 July 2026

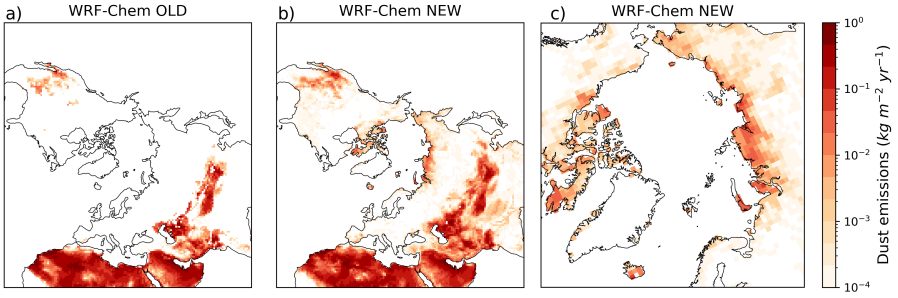

Figure 3. Simulated mineral dust emissions in 2012, in a) WRF-Chem with baseline dust emissions b) WRF-Chem with new dust emissions developed in this study, also showing c) a zoom over the Arctic region.

immersion freezing, and Cooper (1986) for ice nucleation in the deposition mode. These formulations do not include the effect of prognostic aerosols on ice nucleating particles (INP) and primary cloud ice formation.

We perform 3 simulations with the modified version of WRF-Chem-Polar: 1) WRF-Chem-OLD, using the original WRF-GOCART baseline dust emissions; 2) WRF-Chem-NEW, using the new dust emissions developed in this study; 3) WRF-Chem-NEW_NOHLD, using the new dust emissions but without high latitude sources ($> 60°N$). All simulations include the new wet scavenging and sedimentation options developed in this study for GOCART (Sect. 4.1 and 4.2), and the new MODIS land use (Sect. 3.5), to only evaluate the contributions of the different emissions.

6 Model evaluation and results

Using the new version of the model described in Sect. 3 and 4 and the setup described in Sect. 5, here we compare the simulated dust emissions (Sect. 6.1) in WRF-Chem-OLD and WRF-Chem-NEW, and evaluate both simulations with climatological observations of mineral dust aerosol concentrations (Sect. 6.2) and deposition (Sect. 6.3) at the surface in the high latitudes of the Northern Hemisphere. Finally, in Sect. 6.4 we show the impact of the new emissions on quantities relevant for the climate impacts of mineral dust.

6.1 Simulated emissions of mineral dust aerosols

Figure 3 shows the simulated annual dust emission flux in WRF-Chem-OLD and WRF-Chem-NEW. Even though emissions are cut when the ground is frozen, covered in snow, or too humid, high latitude sources are still significant using the new emissions, and total emissions above 60°N go from 0 in WRF-Chem-OLD to 34 $\mathrm{Tg\ yr^{-1}}$ in WRF-Chem-NEW, comparable to the estimate of 48 $\mathrm{Tg\ yr^{-1}}$ from Groot Zwaaftink et al. (2016).

The most intense Arctic emissions are found where the S-function is also strong, for example in Iceland, in the Canadian Archipelago and in Northern Siberia. The only exception is coastal Greenland, where emissions are limited even where the S-function is high, and even though strong dust events are known to be possible (Meinander et al., 2022). This is probably because,

https://doi.org/10.5194/egusphere-2026-4112
Preprint. Discussion started: 21 July 2026

at coarse resolutions, the model cannot reproduce strong winds and dry unfrozen soils in narrow glacial throughs during the warm season. To reproduce an event of this kind in Alaska, Bellamy et al. (2026) had to use a resolution of 600 m and to significantly fine-tune the model surface characterization. These resolutions, and detailed local fine-tuning, are not feasible in a medium- or large- scale model, and simulating these events would likely require the development of advanced subgrid parameterizations to estimate the local conditions in glacial outwash plains from larger-scale variables. It is also possible that glacial dust has different properties than other dust sources, such as a finer size, and that it is able to be mobilized more easily than traditional dust sources. In this case, emissions could also be improved by using better descriptions of soil composition in these regions.

6.2 Simulated concentrations of mineral dust aerosols

We compare on Figure 4 the yearly averaged concentrations of mineral dust aerosol simulated at the surface with the climatological observations of mineral dust aerosols concentrations at the surface available north of 50°N. We use the observations from Checa-Garcia et al. (2021) for the lower latitudes, and Groot Zwaaftink et al. (2016) for Stórhöfði-Heimaey (Iceland, 1997 to 2002). At other high latitude sites, we estimate dust concentrations from aluminum measurements, assuming a mass ratio of 8 % (Prospero, 1999), at Zeppelin (Svalbard, 1996 to 2025; Aas, 2024), Villum (Greenland, 1994 to 2000 and 2008 to 2012; Kemp, 2018), and Alert (Canada, 1983 to 1995; Barrie, 2018). The full data table is also provided at Marelle et al. (2026b), including detailed references for each entry.

We compare the updated WRF-Chem simulations (WRF-Chem-NEW) to the setup with old emissions (WRF-Chem-OLD). We also compare our results to dust concentrations from the CAMS reanalysis (Copernicus Atmosphere Monitoring Service, 2020; Inness et al., 2019), and from the CESM2.2 CAM-Chem simulation used to set initial and boundary conditions in WRF-Chem. It is important to note that, because there are very few mineral dust aerosol observations available in a given year, we compare simulation results for 2012 to longer-term observations from different years, and that a degree of disagreement should be expected due to inter annual variability.

The new mineral dust emissions (WRF-Chem-NEW, Figure 4e,i) strongly improves model results ($R = 0.79$, $RMSE = 0.70$, all measures in log space) compared to the baseline emissions in WRF-Chem-OLD (Figure 4d,h) (log-$R = 0.45$, log-$RMSE = 1.73$), and especially compared to the driving global CESM simulation (Figure 4c,g) (log-$R = 0.43$, log-$RMSE = 2.8$). This is mostly due to improvements at high latitudes. At lower latitudes ($50°N < latitude < 60°N$), WRF-Chem-NEW also has better performance than other models on average, but concentrations are still strongly underestimated (log-$RMSE = 0.72$, corresponding to an underestimation by a factor of 2). This could be because of missing agricultural dust sources, which are not included in any of the models shown here, but could have a large impact in the mid-latitudes (Shi et al., 2025). Although the CAMS reanalysis assimilates aerosol observations and is often considered as a validation dataset for aerosols, Figure 4b,f shows that it struggles to reproduce observed mineral dust concentrations (log-$R = 0.37$, log-$RMSE = 2.6$), and underestimates concentrations more than any of the WRF-Chem setups.

https://doi.org/10.5194/egusphere-2026-4112
Preprint. Discussion started: 21 July 2026

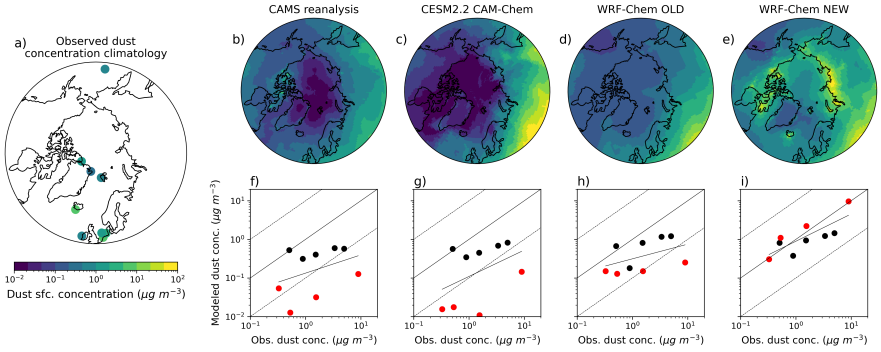

Figure 4. Annual mean surface concentrations of mineral dust: a) observed climatology; b-e) modeled 2012 average; f-i) comparison of climatological observations and of 2012 model results at observation sites. b,f) CAMS reanalysis; c,g) CESM2.2 CAM-Chem global simulation used to drive WRF-Chem initial and boundary conditions; d,h) WRF-Chem with baseline dust emissions; e,i) WRF-Chem with new dust emissions developed in this study. On the scatter plots, red dots indicate Arctic sites (latitude > 60°N).

6.3 Simulated deposition of mineral dust aerosols

We compare on Figure 5 accumulated mineral dust aerosol deposition at the surface in 2012 north of 50°N in WRF-Chem to climatological observations from the datasets of Checa-Garcia et al. (2021) and Huneeus et al. (2011). The full data table is also provided at Marelle et al. (2026b). Only a few measurements are available at higher latitudes, and in the Arctic only in Greenland.

Both WRF-Chem-OLD and WRF-Chem-NEW simulations show comparable and reasonable performance (log-$R = 0.92$ and 0.94, and log-$RMSE = 0.86$ and 0.86, respectively). Both simulations overestimate dust deposition in Greenland, however, the largest differences between simulations are found in Northern Russia, the Canadian Archipelago and in Iceland, where there are no direct observations to evaluate results. Arnalds et al. (2016) found that background dust deposition fluxes in Iceland were 10 to 50 $\mathrm{g\,m^{-2}\,yr^{-1}}$. Deposition in Iceland in WRF-Chem-NEW is 2 to 20 $\mathrm{g\,m^{-2}\,yr^{-1}}$, and in WRF-Chem-OLD less than 0.5 $\mathrm{g\,m^{-2}\,yr^{-1}}$. Modeling Icelandic dust remains a challenge (Groot Zwaaftink et al., 2017; Cvetkovic et al., 2022) and developments should be continued in the future to improve this source.

6.4 Impacts of mineral dust emissions on simulated INP, AOD, and deposition to snow and ice

In this section we will show the impacts of simulated high latitude dust emissions on several measures related to the climate impacts of dust aerosols. The radiative impacts of mineral dust on climate occur mainly through:

- their direct interactions with solar and terrestrial radiation (ARI), which increases with AOD
- their interactions with clouds (ACI), and especially their influence on INP concentrations and ice clouds which remains extremely uncertain

https://doi.org/10.5194/egusphere-2026-4112
Preprint. Discussion started: 21 July 2026

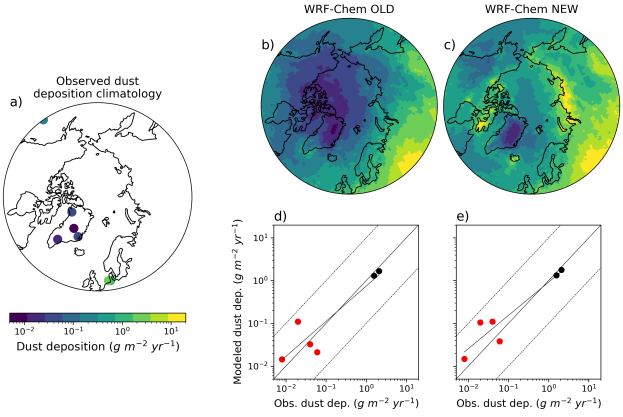

Figure 5. Annual deposition of mineral dust at the surface a) observed long-term climatology b-c) modeled in 2012 d-e) comparison of climatological observations and of 2012 model results at observation sites. b,d) WRF-Chem with baseline dust emissions c,e) WRF-Chem with new dust emissions developed in this study. On the scatter plots, points in red indicate Arctic sites (latitude > 60°N).

– their effect on surface albedo when deposited onto snow and ice, which is related to the total deposition flux to frozen surfaces.

The total simulated deposition of mineral dust aerosols onto snow and ice in 2012 is presented on Figure 6a. Compared to Figure 5c, the deposited dust flux is proportionally stronger in the high Arctic, due to the extensive snow and ice covers nearly year-round. There, high-latitude dust sources are responsible for nearly 100 % of the total deposition to frozen surfaces (Figure 6b), indicating that they could have a disproportionate impact on albedo in the high Arctic. This confirms earlier results from Groot Zwaaftink et al. (2016). It will be possible in future work to include a parameterization of snow and ice albedo that includes the effect of light absorbing impurities (e.g. SNICAR, Flanner et al., 2021, very recently implemented in version 4.8.0 of WRF-Chem) to assess the effect of deposited mineral dust on the radiative budget of the Arctic.

The interactions between aerosols and radiation are related to their optical depth. Figure 6c shows the total AOD in the WRF-Chem-NEW simulation. Even though the aerosol setup does not include any secondary aerosols, the order of magnitude of the simulated AOD is representative of Arctic conditions (between 0.05 and 0.2, Sand et al., 2017; AMAP, 2022). High latitude dust emissions have a clear but limited effect on AOD (Figure 6d, at most 0.01 or $\sim 10\%$ over source regions. These results show that in the future, this setup can be used to diagnose the ARI effect of Arctic dust including high latitude sources.

Mineral dust aerosols are efficient ice nucleating particles (INP) that can initiate the formation of ice clouds. INP could have a disproportionate impact in the Arctic (Matsui et al., 2024), where supercooled liquid clouds and mixed-phase clouds are especially prevalent (Mioche et al., 2015). In the WRF-Chem model, dust INP effects on primary ice formation can be taken into account in the cloud microphysics model of Thompson and Eidhammer (2014), using the formulation of DeMott et al. (2010) to calculate INP:

https://doi.org/10.5194/egusphere-2026-4112
Preprint. Discussion started: 21 July 2026

$$N_{INP} = 5.94 \times 10^{-5}(-T_c)^{3.33} N_{aer0.5}^{-0.0264T_c+0.0033} \quad (18)$$

Where N_{INP} is the number concentration of INP ($\mathrm{standard\,L^{-1}}$), T_c is the air temperature (°C, valid between -35°C and -5°C) and $N_{aer0.5}$ is the number concentration of all aerosols larger than 500 nm ($\mathrm{standard\,cm^{-3}}$), but the WRF implementation only uses the number of dust aerosols above this size. Instead of using climatological dust concentrations as in Thompson and Eidhammer (2014) within WRF-Chem, WRF-Chem-Polar can also use prognostic aerosols from the GOCART or MOSAIC aerosol schemes to set $N_{aer0.5}$ and calculate INP (Marelle et al., 2025)

In WRF-Chem-NEW, we did not include this coupled interaction of prognostic dust on INP and clouds, but we can re-calculate *a posteriori* the concentration of INP using Eq. 18. We show on Figure 6e the yearly averaged INP column from WRF-Chem-NEW at -20°C, a temperature typical of dust INP activity. The amounts are relatively low in the Arctic compared to continental regions at lower latitudes, with typical Arctic surface concentrations of 0.1 to 1 $\mathrm{L^{-1}}$ (Li et al., 2022). Adding high-latitude dust sources only has a modest effect on the total INP column, at most 20% (Figure 6f). This is partly due to the form of Eq. 18, which is non linear: a 10× increase in aerosols only leads to 3.4× more INP. More up-to-date surface-area-based formulations (e.g., Niemand et al., 2012; Ullrich et al., 2017) could be more linearly sensitive to dust aerosols.

In addition to the impacts illustrated on Figure 6, mineral dust aerosols could also have an important effect on liquid clouds, because Arctic aerosols are often internally mixed with hydrophilic compounds (Kirpes et al., 2018), and large particles such as dust usually constitute better CCN. In addition, dust has been shown to strongly influence atmospheric chemistry and even biological activity (Kok et al., 2023)). These effects were not investigated specifically here, but could be modeled using the MOSAIC aerosol setup in WRF-Chem-Polar also compatible with our developments, and our study lays the groundwork for a future investigation of the full range of impacts of Arctic dust on climate (ARI, ACI, snow albedo, chemistry, and biology).

7 Discussion and conclusions

We created a new version of the WRF-Chem-Polar model with modified emissions and sinks of mineral dust aerosols, and including previously missing high latitude sources, available at Marelle et al. (2026c). The upgraded model compares well to observed dust surface concentrations and deposition, and improves on the original WRF-Chem model and on a state-of-the-art global model and reanalysis, in the Arctic and in the northern mid-latitudes. However, because of the relative paucity of direct observations of mineral dust in the Arctic, constraining the model remains a challenge. It would be very useful if future observation campaigns could measure dust aerosol concentrations and deposition in the high Arctic, where our model predicts they are the most sensitive to high-latitude sources. For example, we find that high latitude sources are responsible for nearly 100 % of dust deposition over Arctic Ocean sea ice, and 10 % of AOD close to emission sources in Northen Siberia, Iceland and the Canadian Archipelago. Observations close to these regions would be especially interesting, ideally in locations sufficiently removed from local sources to sample regional background concentrations.

The model is able to represent the effect of mineral dust aerosols on radiation and clouds, and can be used in the future to better quantify the impacts of dust on the Arctic climate. The current configuration of the model is able to represent the effect

https://doi.org/10.5194/egusphere-2026-4112
Preprint. Discussion started: 21 July 2026

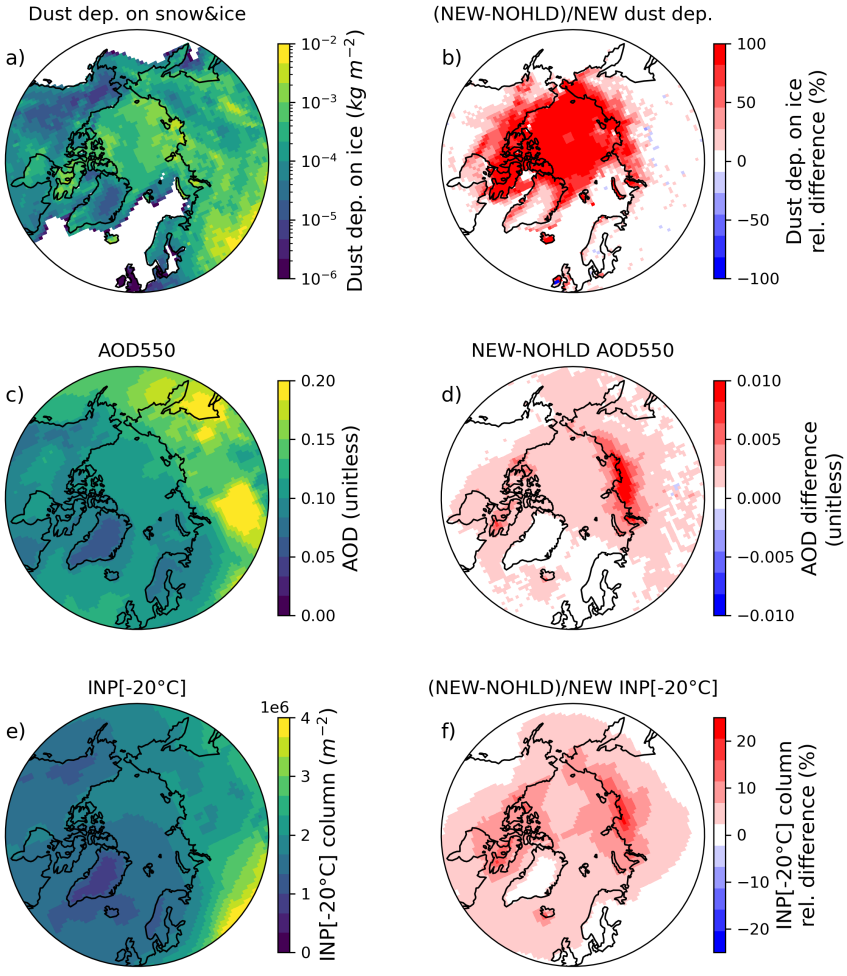

Figure 6. Effect of high latitude dust emissions on: a,b) dust deposition on snow and ice; c,d) Aerosol Optical Depth (AOD) at 550 nm; e,f) total column of Ice Nucleating Particle (INP) number at -20°C. Left: Annual mean WRF-Chem model results with the new dust emissions developed in this study. Right: Contributions from high latitude dust emissions, calculated by comparing WRF-Chem-NEW with WRF-Chem-NEW_NOHLD.

of aerosol-cloud interactions (ACI) on liquid, ice, and mixed-phase clouds, but the representation of INP and their effect on primary ice formation in the model is outdated and will have to be further tested and improved for an accurate representation of ACI. Generally speaking, optical properties, INP activity, and size distributions of high latitude dust could be very different than in other regions (Di Biagio et al., 2026; Matsui et al., 2024) and the sensitivity to these parameters will need to be explored.

https://doi.org/10.5194/egusphere-2026-4112
Preprint. Discussion started: 21 July 2026

The model predicts that high latitude dust has a major impact on dust deposition fluxes onto snow and ice. The associated radiative effect can be calculated using a snow albedo model, and some of them already implemented in other versions of WRF-Chem that can be integrated into our version for evaluating these effects.

While our new dust emissions represents a significant progress, we believe there is still room for improvement. For example, recent studies indicate that emissions of agricultural dust in the mid-latitudes, not represented in WRF-Chem or in almost any other model (Shi et al., 2025), could be transported to the Arctic (Ansmann et al., 2023; Raif et al., 2024). In addition, the seasonal variation of the bare soil fraction in WRF-Chem, used to scale emissions in regions with partially bare soil in our model, is based on a monthly, fixed climatology. Using more resolved time-varying vegetation data instead would certainly improve the simulated temporal variation of these emissions. Last but not least, we found that mineral dust emissions from glacial outwash plains in Greenland are probably underestimated by our model, either because local conditions in complex topography cannot be resolved directly in a large scale model, or because their properties are different and they could be mobilized more easily than other sources. It would be necessary to improve their description, with more up-to-date soil composition data in the Arctic or with additional sub-grid parameters to estimate local meteorological conditions in this complex terrain.

The new FORTRAN modules created for this study (for dust emissions, aerosol sedimentation, and wet scavenging) were written to be as model-agnostic as possible, in order to be more easily portable to other models than WRF-Chem. To facilitate this, we also provide an offline version of the modules that can be run outside of WRF-Chem, and the associated test programs, at Marelle et al. (2026a). In addition, the emission module developed in this study is structured to be easily modified to include other recent formulations of mineral dust aerosol emissions (e.g., Shao et al., 2011; Kok et al., 2014; Groot Zwaaftink et al., 2017; LeGrand et al., 2023), and could serve as a basis for a future intercomparison of these emission models in a single model framework, in the Arctic or elsewhere.

The model version developed in this study was not specifically tuned for the northern high latitudes, and it can be used to investigate other regions, such as Antarctica where dust aerosol can be transported from the southern midlatitudes, (Lapere et al., 2024b), or even outside of the poles, where dust transport events from major deserts can degrade air quality and influence the predictions of weather models.

Code and data availability. We provide the updated WRF-Chem-Polar model version used in this study as Marelle et al. (2026c). Standalone "offline" versions of the 3 new WRF-Chem-Polar modules created for this study for dust emissions, aerosol sedimentation, and wet scavenging, are also provided as Marelle et al. (2026a) so that they can be tested without running coupled WRF-Chem runs, and can be more easily integrated in different models if needed. The S-function (erodibility) source term for dust emissions created for this study can be obtained from Marelle (2026b), also including the associated preprocessing scripts needed to regenerate it from ETOPO 2022 elevation data (available at NOAA National Centers for Environmental Information, 2022) and the GLCNMOv3 land cover dataset (https://archive.softwareheritage.org/browse/snapshot/ce449a02d46d67d5cef07ef842d41bde9b5246e4/directory/?origin_url=https://github.com/globalmaps/gm_lc_v3. The WRF preprocessing system (WPS) version 4 is available at https://archive.softwareheritage.org/swh:1:snp:096256316e752343901abad92a7dd9c2529f48cb;origin=https://github.com/wrf-model/WPS. The new land cover dataset for WPS modis_landuse_20class_3m_with_lakes and the configuration files required to use it in WPS are available at Marelle (2026a), as well as the scripts needed to regenerate it from the MODIS

https://doi.org/10.5194/egusphere-2026-4112
Preprint. Discussion started: 21 July 2026

MCD12C1.061 land cover (available at Friedl and Sulla-Menashe, 2022) and from Natural Earth Data lake shapefiles (https://www.naturalearthdata.com/downloads/10m-physical-vectors/10m-lakes/, last accessed 2026-07-03).

WRF-Chem preprocessor tools (mozbc, fire_emiss and bio_emiss) are available at https://www2.acom.ucar.edu/wrf-chem/wrf-chem-tools-community. We also provide the WRF-Chem namelists, run and setup scripts for the simulations presented here, as well as the preprocessing codes, post-processing codes, and figure data associated to this study as Marelle et al. (2026b). ERA5 input data on pressure and surface levels for WRF are available at Copernicus Climate Change Service (2017), and the CESM CAM-Chem input data for initial and boundary conditions at Tilmes et al. (2022). The CAMS reanalysis is available at Copernicus Atmosphere Monitoring Service (2020). The ECLIPSE V6b anthropogenic emissions can be obtained from https://iiasa.ac.at/models-tools-data/global-emission-fields-of-air-pollutants-and-ghgs (last accessed: 2026-07-03) FINNv2.5 emissions are available at https://doi.org/10.5281/zenodo.7868652. Aluminum measurements at Zeppelin (Svalbard), Villum (Greenland), and Alert (Canada) can be obtained at Aas (2024) Kemp (2018) and Barrie (2018) respectively. Dust concentration and deposition data are available in the supplements of Checa-Garcia et al. (2021) and Huneeus et al. (2011), and were reproduced in Marelle et al. (2026b).

Author contributions. Conceptualization: LM; Data curation: all authors; Formal analysis: LM, RL; Funding acquisition: LM, JLT; Investigation: LM, ADS; Methodology: LM, ADS; Project administration: LM; Resources: LM, JLT; Software: All authors; Supervision: LM, JLT; Validation: all authors; Visualization: LM; Writing (original draft preparation): all authors; Writing (review and editing): all authors.

Competing interests. The authors declare no competing interests.

Acknowledgements. This project has received funding from the Horizon Europe programme under Grant 101137680 via project CERTAINTY (Cloud-aERosol inTeractions & their impActs IN The earth sYstem); and from the Simons Foundation through the project Assessing Cirrus Cloud Thinning Strategies by Learning from Aerosol-Cirrus Interactions in Natural and Perturbed Conditions. Computer analyses benefited from access to IDRIS HPC resources (GENCI allocations A015017141, A017017141 and A019017141), and from the IPSL Data and Computing Center ESPRI which is supported by CNRS, SU, CNES and Ecole Polytechnique. We acknowledge the use of the WRF-Chem preprocessor tools mozbc and fire_emiss provided by the Atmospheric Chemistry Observations and Modeling Lab (ACOM) of NCAR. Observational aluminium concentration data used in this study were accessed from EBAS (https://ebas.nilu.no) hosted by NILU. We acknowledge the Geospatial Information Authority of Japan, Chiba University and collaborating organizations for the GLCNMOv3 land cover dataset.

https://doi.org/10.5194/egusphere-2026-4112
Preprint. Discussion started: 21 July 2026

References

Aas, W.: Measurement of Heavy metals at Zeppelin mountain (Ny-Ålesund), https://doi.org/10.48597/RBKK-FSDT, 2024.

Ahmed, S., Thomas, J. L., Angot, H., Dommergue, A., Archer, S. D., Bariteau, L., Beck, I., Benavent, N., Blechschmidt, A.-M., Blomquist, B., Boyer, M., Christensen, J. H., Dahlke, S., Dastoor, A., Helmig, D., Howard, D., Jacobi, H.-W., Jokinen, T., Lapere, R., Laurila, T., Quéléver, L. L. J., Richter, A., Ryjkov, A., Mahajan, A. S., Marelle, L., Pfaffhuber, K. A., Posman, K., Rinke, A., Saiz-Lopez, A., Schmale, J., Skov, H., Steffen, A., Stupple, G., Stutz, J., Travnikov, O., and Zilker, B.: Modelling the coupled mercury-halogen-ozone cycle in the central Arctic during spring, Elementa: Science of the Anthropocene, 11, https://doi.org/10.1525/elementa.2022.00129, 00129, 2023.

AMAP: AMAP Assessment 2021: Impacts of Short-lived Climate Forcers on Arctic Climate, Air Quality, and Human Health, Arctic Monitoring and Assessment Programme (AMAP), Tromsø, Norway, https://www.amap.no/documents/doc/amap-assessment-2021-impacts-of-short-lived-climate-forcers-on-arctic-climate-air-quality-and-human-health/3614, 2022.

Ansmann, A., Ohneiser, K., Engelmann, R., Radenz, M., Griesche, H., Hofer, J., Althausen, D., Creamean, J. M., Boyer, M. C., Knopf, D. A., Dahlke, S., Maturilli, M., Gebauer, H., Bühl, J., Jimenez, C., Seifert, P., and Wandinger, U.: Annual cycle of aerosol properties over the central Arctic during MOSAiC 2019–2020 – light-extinction, CCN, and INP levels from the boundary layer to the tropopause, Atmospheric Chemistry and Physics, 23, 12 821–12 849, https://doi.org/10.5194/acp-23-12821-2023, 2023.

Arnalds, O., Dagsson-Waldhauserova, P., and Olafsson, H.: The Icelandic volcanic aeolian environment: Processes and impacts — A review, Aeolian Research, 20, 176–195, https://doi.org/https://doi.org/10.1016/j.aeolia.2016.01.004, 2016.

Barrie, L.: Measurement of Heavy metals at Alert, https://doi.org/10.48597/26WM-2Q56, 2018.

Bellamy, D., Klose, M., Nadeau, D. F., Engelstaedter, S., Washington, R., and King, J.: Modelling mineral dust emissions from proglacial valleys of the St. Elias Mountains, Canada, EGUsphere, 2026, 1–40, https://doi.org/10.5194/egusphere-2026-1343, 2026.

Bigg, E. K.: The Supercooling of Water, Proceedings of the Physical Society. Section B, 66, 688, https://doi.org/10.1088/0370-1301/66/8/309, 1953.

Checa-Garcia, R., Balkanski, Y., Albani, S., Bergman, T., Carslaw, K., Cozic, A., Dearden, C., Marticorena, B., Michou, M., van Noije, T., Nabat, P., O'Connor, F. M., Olivié, D., Prospero, J. M., Le Sager, P., Schulz, M., and Scott, C.: Evaluation of natural aerosols in CRESCENDO Earth system models (ESMs): mineral dust, Atmospheric Chemistry and Physics, 21, 10 295–10 335, https://doi.org/10.5194/acp-21-10295-2021, 2021.

Chin, M., Ginoux, P., Kinne, S., Torres, O., Holben, B. N., Duncan, B. N., Martin, R. V., Logan, J. A., Higurashi, A., and Nakajima, T.: Tropospheric Aerosol Optical Thickness from the GOCART Model and Comparisons with Satellite and Sun Photometer Measurements, J. Atmos. Sci., 59, 461–483, https://doi.org/10.1175/1520-0469(2002)059<0461:TAOTFT>2.0.CO;2, 2002.

Cooper, W. A.: Ice Initiation in Natural Clouds, Meteorological Monographs, 21, 29 – 32, https://doi.org/10.1175/0065-9401-21.43.29, 1986.

Copernicus Atmosphere Monitoring Service: CAMS global reanalysis (EAC4)[Dataset], http://doi.org/10.24381/d58bbf47, accessed 9-June-2026, 2020.

Copernicus Climate Change Service: ERA5: Fifth generation of ECMWF atmospheric reanalyses of the global climate [Dataset], http://doi.org/10.24381/cds.adbb2d47, accessed 11-May-2021, 2017.

Cvetkovic, B., Dagsson-Waldhauserov'a, P., Petkovic, S., Arnalds, O., Madonna, F., Proestakis, E., Gkikas, A., Vukovic Vimic, A., Pejanovic, G., Rosoldi, M., Ceburnis, D., Amiridis, V., Lis'a, L., Nickovic, S., and Nikolic, J.: Fully Dynamic High–Resolution Model for Dispersion of Icelandic Airborne Mineral Dust, Atmosphere, 13, https://doi.org/10.3390/atmos13091345, 2022.

https://doi.org/10.5194/egusphere-2026-4112
Preprint. Discussion started: 21 July 2026

DeMott, P. J., Prenni, A. J., Liu, X., Kreidenweis, S. M., Petters, M. D., Twohy, C. H., Richardson, M. S., Eidhammer, T., and Rogers, D. C.: Predicting global atmospheric ice nuclei distributions and their impacts on climate, Proceedings of the National Academy of Sciences, 107, 11 217–11 222, https://doi.org/10.1073/pnas.0910818107, 2010.

Després, B. and Lagoutière, F.: Un schéma non linéaire anti-dissipatif pour l'équation d'advection linéaire, Comptes Rendus de l'Académie des Sciences - Series I - Mathematics, 328, 939–943, https://doi.org/https://doi.org/10.1016/S0764-4442(99)80301-2, 1999.

Di Biagio, C., Bru, E., Orta, A., Chevaillier, S., Baldo, C., Bergé, A., Cazaunau, M., Lafon, S., Nowak, S., Pangui, E., Andreae, M. O., Dagsson-Waldhauserova, P., Dintwe, K., Kandler, K., King, J. S., Chaput, A., Okin, G. S., Piketh, S., Saeed, T., Seibert, D., Shi, Z., Williams, E., Sellitto, P., and Formenti, P.: Mid- and far-infrared spectral signatures of mineral dust from low- to high-latitude regions: significance and implications, Atmospheric Chemistry and Physics, 26, 1079–1091, https://doi.org/10.5194/acp-26-1079-2026, 2026.

Drakaki, E., Amiridis, V., Tsekeri, A., Gkikas, A., Proestakis, E., Mallios, S., Solomos, S., Spyrou, C., Marinou, E., Ryder, C. L., Bouris, D., and Katsafados, P.: Modeling coarse and giant desert dust particles, Atmospheric Chemistry and Physics, 22, 12 727–12 748, https://doi.org/10.5194/acp-22-12727-2022, 2022.

Drakaki, E., Mallios, S., García-Pando, C. P., Katsafados, P., and Amiridis, V.: Small but Notable Influence of Numerical Diffusion on Super Coarse Dust Sedimentation: Insights from UNO3 vs. Upwind Schemes, Atmosphere, 16, https://doi.org/10.3390/atmos16091086, 2025.

Fécan, F., Marticorena, B., and Bergametti, G.: Parametrization of the increase of the aeolian erosion threshold wind friction velocity due to soil moisture for arid and semi-arid areas, Annales Geophysicae, 17, 149–157, https://doi.org/10.1007/s00585-999-0149-7, 1999.

Flanner, M. G., Arnheim, J. B., Cook, J. M., Dang, C., He, C., Huang, X., Singh, D., Skiles, S. M., Whicker, C. A., and Zender, C. S.: SNICAR-ADv3: a community tool for modeling spectral snow albedo, Geoscientific Model Development, 14, 7673–7704, https://doi.org/10.5194/gmd-14-7673-2021, 2021.

Friedl, M. and Sulla-Menashe, D.: MODIS/Terra+Aqua Land Cover Type Yearly L3 Global 0.05Deg CMG V061 [Dataset], http://10.5067/MODIS/MCD12C1.061, accessed 10-June-2026, 2022.

Ginoux, P., Chin, M., Tegen, I., Prospero, J. M., Holben, B., Dubovik, O., and Lin, S.-J.: Sources and distributions of dust aerosols simulated with the GOCART model, Journal of Geophysical Research: Atmospheres, 106, 20 255–20 273, https://doi.org/https://doi.org/10.1029/2000JD000053, 2001.

Ginoux, P., Prospero, J., Torres, O., and Chin, M.: Long-term simulation of global dust distribution with the GOCART model: correlation with North Atlantic Oscillation, Environmental Modelling & Software, 19, 113–128, https://doi.org/https://doi.org/10.1016/S1364-8152(03)00114-2, modelling of Wind Erosion and Aeolian Processes, 2004.

Grell, G. A. and Dévényi, D.: A generalized approach to parameterizing convection combining ensemble and data assimilation techniques, Geophysical Research Letters, 29, 38–1–38–4, https://doi.org/10.1029/2002GL015311, 2002.

Grell, G. A., Peckham, S. E., Schmitz, R., McKeen, S. A., Frost, G., Skamarock, W. C., and Eder, B.: Fully coupled "online" chemistry within the WRF model, Atmospheric Environment, 39, 6957–6975, https://doi.org/http://dx.doi.org/10.1016/j.atmosenv.2005.04.027, 2005.

Groot Zwaaftink, C. D., Grythe, H., Skov, H., and Stohl, A.: Substantial contribution of northern high-latitude sources to mineral dust in the Arctic, Journal of Geophysical Research: Atmospheres, 121, 13,678–13,697, https://doi.org/https://doi.org/10.1002/2016JD025482, 2016.

Groot Zwaaftink, C. D., Arnalds, O., Dagsson-Waldhauserova, P., Eckhardt, S., Prospero, J. M., and Stohl, A.: Temporal and spatial variability of Icelandic dust emissions and atmospheric transport, Atmospheric Chemistry and Physics, 17, 10 865–10 878, https://doi.org/10.5194/acp-17-10865-2017, 2017.

https://doi.org/10.5194/egusphere-2026-4112
Preprint. Discussion started: 21 July 2026

Huneeus, N., Schulz, M., Balkanski, Y., Griesfeller, J., Prospero, J., Kinne, S., Bauer, S., Boucher, O., Chin, M., Dentener, F., Diehl, T., Easter, R., Fillmore, D., Ghan, S., Ginoux, P., Grini, A., Horowitz, L., Koch, D., Krol, M. C., Landing, W., Liu, X., Mahowald, N., Miller, R., Morcrette, J.-J., Myhre, G., Penner, J., Perlwitz, J., Stier, P., Takemura, T., and Zender, C. S.: Global dust model intercomparison in AeroCom phase I, Atmospheric Chemistry and Physics, 11, 7781–7816, https://doi.org/10.5194/acp-11-7781-2011, 2011.

Iacono, M. J., Delamere, J. S., Mlawer, E. J., Shephard, M. W., Clough, S. A., and Collins, W. D.: Radiative forcing by long-lived greenhouse gases: Calculations with the AER radiative transfer models, Journal of Geophysical Research: Atmospheres, 113, https://doi.org/10.1029/2008JD009944, d13103, 2008.

Inness, A., Ades, M., Agustí-Panareda, A., Barré, J., Benedictow, A., Blechschmidt, A.-M., Dominguez, J. J., Engelen, R., Eskes, H., Flemming, J., Huijnen, V., Jones, L., Kipling, Z., Massart, S., Parrington, M., Peuch, V.-H., Razinger, M., Remy, S., Schulz, M., and Suttie, M.: The CAMS reanalysis of atmospheric composition, Atmospheric Chemistry and Physics, 19, 3515–3556, https://doi.org/10.5194/acp-19-3515-2019, 2019.

Ioannidis, E., Law, K. S., Raut, J.-C., Marelle, L., Onishi, T., Kirpes, R. M., Upchurch, L. M., Tuch, T., Wiedensohler, A., Massling, A., Skov, H., Quinn, P. K., and Pratt, K. A.: Modelling wintertime sea-spray aerosols under Arctic haze conditions, Atmospheric Chemistry and Physics, 23, 5641–5678, https://doi.org/10.5194/acp-23-5641-2023, 2023.

Ioannidis, E., Law, K. S., Raut, J.-C., Marelle, L., Onishi, T., Andrews, E., Ohata, S., Mori, T., Morris, S., Kondo, Y., Sharma, S., Eleftheriadis, K., Klimont, Z., Soulie, A., Granier, C., Quinn, P. K., and Pratt, K. A.: Sensitivity of Wintertime Arctic Black Carbon to Removal Processes and Regional Alaskan Sources, Journal of Geophysical Research: Atmospheres, 130, e2024JD042 885, https://doi.org/https://doi.org/10.1029/2024JD042885, 2025.

Jickells, T. D., An, Z. S., Andersen, K. K., Baker, A. R., Bergametti, G., Brooks, N., Cao, J. J., Boyd, P. W., Duce, R. A., Hunter, K. A., Kawahata, H., Kubilay, N., laRoche, J., Liss, P. S., Mahowald, N., Prospero, J. M., Ridgwell, A. J., Tegen, I., and Torres, R.: Global Iron Connections Between Desert Dust, Ocean Biogeochemistry, and Climate, Science, 308, 67–71, https://doi.org/10.1126/science.1105959, 2005.

Kawai, K., Matsui, H., and Tobo, Y.: Dominant Role of Arctic Dust With High Ice Nucleating Ability in the Arctic Lower Troposphere, Geophysical Research Letters, 50, e2022GL102 470, https://doi.org/https://doi.org/10.1029/2022GL102470, e2022GL102470 2022GL102470, 2023.

Kelso, N. V. and Patterson, T.: Introducing Natural Earth Data - naturalearthdata.com, Geographia Technica, 5, 25, 2010.

Kemp, K.: Measurement of Heavy metals at Villum Research Station, Station Nord, https://doi.org/10.48597/8QWV-NWA5, 2018.

Kirpes, R. M., Bondy, A. L., Bonanno, D., Moffet, R. C., Wang, B., Laskin, A., Ault, A. P., and Pratt, K. A.: Secondary sulfate is internally mixed with sea spray aerosol and organic aerosol in the winter Arctic, Atmospheric Chemistry and Physics, 18, 3937–3949, https://doi.org/10.5194/acp-18-3937-2018, 2018.

Klimont, Z., Kupiainen, K., Heyes, C., Purohit, P., Cofala, J., Rafaj, P., Borken-Kleefeld, J., and Schöpp, W.: Global anthropogenic emissions of particulate matter including black carbon, Atmospheric Chemistry and Physics, 17, 8681–8723, https://doi.org/10.5194/acp-17-8681-2017, 2017.

Kobayashi, T., Tateishi, R., Alsaaideh, B., Sharma, R., Wakaizumi, T., Miyamoto, D., Bai, X., Long, B., Gegentana, G., and Maitiniyazi, A.: Production of Global Land Cover Data - GLCNMO2013, Journal of Geography and Geology, 9, 1–15, https://doi.org/http://dx.doi.org/10.5539/jgg.v9n3p1, 2017.

Kok, J. F.: A scaling theory for the size distribution of emitted dust aerosols suggests climate models underestimate the size of the global dust cycle, Proceedings of the National Academy of Sciences, 108, 1016–1021, https://doi.org/10.1073/pnas.1014798108, 2011.

https://doi.org/10.5194/egusphere-2026-4112
Preprint. Discussion started: 21 July 2026

Kok, J. F., Mahowald, N. M., Fratini, G., Gillies, J. A., Ishizuka, M., Leys, J. F., Mikami, M., Park, M.-S., Park, S.-U., Van Pelt, R. S., and Zobeck, T. M.: An improved dust emission model – Part 1: Model description and comparison against measurements, Atmospheric Chemistry and Physics, 14, 13 023–13 041, https://doi.org/10.5194/acp-14-13023-2014, 2014.

Kok, J. F., Adebiyi, A. A., Albani, S., Balkanski, Y., Checa-Garcia, R., Chin, M., Colarco, P. R., Hamilton, D. S., Huang, Y., Ito, A., Klose, M., Li, L., Mahowald, N. M., Miller, R. L., Obiso, V., Pérez García-Pando, C., Rocha-Lima, A., and Wan, J. S.: Contribution of the world's main dust source regions to the global cycle of desert dust, Atmospheric Chemistry and Physics, 21, 8169–8193, https://doi.org/10.5194/acp-21-8169-2021, 2021.

Kok, J. F., Storelvmo, T., Karydis, V. A., Adebiyi, A. A., Mahowald, N. M., Evan, A. T., He, C., and Leung, D. M.: Mineral dust aerosol impacts on global climate and climate change, Nature Reviews Earth & Environment, 4, 71–86, https://doi.org/10.1038/s43017-022-00379-5, 2023.

Kok, J. F., K. Gupta, A., Evan, A. T., Pérez García-Pando, C., Li, L., Adebiyi, A. A., Albani, S., Balkanski, Y., Checa-Garcia, R., Colarco, P. R., Hamilton, D. S., Huang, Y., Ito, A., Klose, M., Mahowald, N. M., Miller, R. L., Obiso, V., Rocha Lima, A., and Wan, J.: Desert dust exerts twice the longwave radiative heating estimated by climate models, Nature Communications, 17, 3191, https://doi.org/10.1038/s41467-026-70952-9, 2026.

Lapere, R., Marelle, L., Rampal, P., Brodeau, L., Melsheimer, C., Spreen, G., and Thomas, J. L.: Modeling the contribution of leads to sea spray aerosol in the high Arctic, Atmospheric Chemistry and Physics, 24, 12 107–12 132, https://doi.org/10.5194/acp-24-12107-2024, 2024a.

Lapere, R., Thomas, J. L., Favier, V., Angot, H., Asplund, J., Ekman, A. M. L., Marelle, L., Raut, J.-C., Da Silva, A., Wille, J. D., and Zieger, P.: Polar Aerosol Atmospheric Rivers: Detection, Characteristics, and Potential Applications, Journal of Geophysical Research: Atmospheres, 129, e2023JD039 606, https://doi.org/https://doi.org/10.1029/2023JD039606, e2023JD039606 2023JD039606, 2024b.

Lapere, R., Haddon, A., Price, R., Marelle, L., Monahan, A. H., Steiner, N., Raut, J., Bastien, L., Willis, M. D., and Thomas, J. L.: Marine secondary aerosols are required for modeling clouds in the Arctic, Geophysical Research Letters, https://doi.org/10.1029/2026GL121724, 2026.

Le Gars, Y., Raut, J.-C., and Marelle, L.: What surface radiative fluxes reveal about Arctic cloud modelling accuracy, EGUsphere, 2026, 1–28, https://doi.org/10.5194/egusphere-2026-2516, 2026.

LeGrand, S. L., Polashenski, C., Letcher, T. W., Creighton, G. A., Peckham, S. E., and Cetola, J. D.: The AFWA dust emission scheme for the GOCART aerosol model in WRF-Chem v3.8.1, Geoscientific Model Development, 12, 131–166, https://doi.org/10.5194/gmd-12-131-2019, 2019.

LeGrand, S. L., Letcher, T. W., Okin, G. S., Webb, N. P., Gallagher, A. R., Dhital, S., Hodgdon, T. S., Ziegler, N. P., and Michaels, M. L.: Application of a satellite-retrieved sheltering parameterization (v1.0) for dust event simulation with WRF-Chem v4.1, Geoscientific Model Development, 16, 1009–1038, https://doi.org/10.5194/gmd-16-1009-2023, 2023.

Li, G., Wieder, J., Pasquier, J. T., Henneberger, J., and Kanji, Z. A.: Predicting atmospheric background number concentration of ice-nucleating particles in the Arctic, Atmospheric Chemistry and Physics, 22, 14 441–14 454, https://doi.org/10.5194/acp-22-14441-2022, 2022.

Listowski, C., Delanoë, J., Kirchgaessner, A., Lachlan-Cope, T., and King, J.: Antarctic clouds, supercooled liquid water and mixed phase, investigated with DARDAR: geographical and seasonal variations, Atmospheric Chemistry and Physics, 19, 6771–6808, https://doi.org/10.5194/acp-19-6771-2019, 2019.

https://doi.org/10.5194/egusphere-2026-4112
Preprint. Discussion started: 21 July 2026

Luo, G., Yu, F., and Schwab, J.: Revised treatment of wet scavenging processes dramatically improves GEOS-Chem 12.0.0 simulations of surface nitric acid, nitrate, and ammonium over the United States, Geoscientific Model Development, 12, 3439–3447, https://doi.org/10.5194/gmd-12-3439-2019, 2019.

Luo, G., Yu, F., and Moch, J. M.: Further improvement of wet process treatments in GEOS-Chem v12.6.0: impact on global distributions of aerosols and aerosol precursors, Geoscientific Model Development, 13, 2879–2903, https://doi.org/10.5194/gmd-13-2879-2020, 2020.

Maillard, J., Raut, J.-C., and Ravetta, F.: Evaluation and development of surface layer scheme representation of temperature inversions over boreal forests in Arctic wintertime conditions, Geoscientific Model Development, 17, 3303–3320, https://doi.org/10.5194/gmd-17-3303-2024, 2024.

Mailler, S., Pennel, R., Menut, L., and Lachâtre, M.: Using the Després and Lagoutière (1999) antidiffusive transport scheme: a promising and novel method against excessive vertical diffusion in chemistry-transport models, Geoscientific Model Development, 14, 2221–2233, https://doi.org/10.5194/gmd-14-2221-2021, 2021.

Marelle, L.: Dominant land cover classification at 0.05 deg for the WRF model, based on MODIS MCD12C1.061 and Natural Earth Data, converted to the WRF geog format, https://doi.org/10.5281/zenodo.21263737, 2026a.

Marelle, L.: S-Function / soil erodibility / dust source function for mineral dust aerosol emissions, including high latitude sources, https://doi.org/10.5281/zenodo.21263226, 2026b.

Marelle, L., Raut, J.-C., Thomas, J. L., Law, K. S., Quennehen, B., Ancellet, G., Pelon, J., Schwarzenboeck, A., and Fast, J. D.: Transport of anthropogenic and biomass burning aerosols from Europe to the Arctic during spring 2008, Atmospheric Chemistry and Physics, 15, 3831–3850, https://doi.org/https://doi.org/10.5194/acp-15-3831-2015, 2015.

Marelle, L., Thomas, J. L., Raut, J.-C., Law, K. S., Jalkanen, J.-P., Johansson, L., Roiger, A., Schlager, H., Kim, J., Reiter, A., and Weinzierl, B.: Air quality and radiative impacts of Arctic shipping emissions in the summertime in northern Norway: from the local to the regional scale, Atmospheric Chemistry and Physics, 16, 2359–2379, https://doi.org/https://doi.org/10.5194/acp-16-2359-2016, 2016.

Marelle, L., Raut, J.-C., Law, K. S., Berg, L. K., Fast, J. D., Easter, R. C., Shrivastava, M., and Thomas, J. L.: Improvements to the WRF-Chem 3.5.1 model for quasi-hemispheric simulations of aerosols and ozone in the Arctic, Geoscientific Model Development, 10, 3661–3677, https://doi.org/10.5194/gmd-10-3661-2017, 2017.

Marelle, L., Thomas, J. L., Ahmed, S., Tuite, K., Stutz, J., Dommergue, A., Simpson, W. R., Frey, M. M., and Baladima, F.: Implementation and Impacts of Surface and Blowing Snow Sources of Arctic Bromine Activation Within WRF-Chem 4.1.1, Journal of Advances in Modeling Earth Systems, 13, e2020MS002 391, https://doi.org/https://doi.org/10.1029/2020MS002391, 2021.

Marelle, L., Myhre, G., Thomas, J. L., and Raut, J.-C.: Aerosol Background Concentrations Influence Aerosol-Cloud Interactions as Much as the Choice of Aerosol-Cloud Parameterization, Geophysical Research Letters, 52, e2024GL111 780, https://doi.org/https://doi.org/10.1029/2024GL111780, 2025.

Marelle, L., Da Silva, A., Lapere, R., Price, R., Bastien, L., and Thomas, J.: Offline modules related to mineral dust aerosols from the WRF-Chem-Polar model, for aerosol sedimentation, wet scavenging, and mineral dust aerosol emissions, https://doi.org/10.5281/zenodo.21264040, 2026a.

Marelle, L., Lapere, R., Da Silva, A., Price, R., Bastien, L., and Thomas, J.: WRF-Chem-Polar configuration files, Figure data, pre- and post-processing scripts for the study of high latitude dust emissions, https://doi.org/10.5281/zenodo.21263932, 2026b.

Marelle, L., Lapere, R., Da Silva, A., Price, R., Bastien, L., and Thomas, J.: WRF-Chem-Polar (WRF-Chem 4.6.1) with modifications for high-latitude dust emissions, https://doi.org/10.5281/zenodo.21292706, 2026c.

https://doi.org/10.5194/egusphere-2026-4112
Preprint. Discussion started: 21 July 2026

Marelle, L., Lapere, R., Price, R., Bastien, L., and Thomas, J.: WRF-Chem-Polar/WRF-Chem-Polar: Price et al., 2026, [Software], https://doi.org/10.5281/zenodo.19736986, 2026d.

Marticorena, B. and Bergametti, G.: Modeling the atmospheric dust cycle: 1. Design of a soil-derived dust emission scheme, Journal of Geophysical Research: Atmospheres, 100, 16 415–16 430, https://doi.org/https://doi.org/10.1029/95JD00690, 1995.

Matsui, H., Kawai, K., Tobo, Y., Iizuka, Y., and Matoba, S.: Increasing Arctic dust suppresses the reduction of ice nucleation in the Arctic lower troposphere by warming, npj Climate and Atmospheric Science, 7, 266, https://doi.org/10.1038/s41612-024-00811-1, 2024.

Meinander, O., Dagsson-Waldhauserova, P., Amosov, P., Aseyeva, E., Atkins, C., Baklanov, A., Baldo, C., Barr, S. L., Barzycka, B., Benning, L. G., Cvetkovic, B., Enchilik, P., Frolov, D., Gassó, S., Kandler, K., Kasimov, N., Kavan, J., King, J., Koroleva, T., Krupskaya, V., Kulmala, M., Kusiak, M., Lappalainen, H. K., Laska, M., Lasne, J., Lewandowski, M., Luks, B., McQuaid, J. B., Moroni, B., Murray, B., Möhler, O., Nawrot, A., Nickovic, S., O'Neill, N. T., Pejanovic, G., Popovicheva, O., Ranjbar, K., Romanias, M., Samonova, O., Sanchez-Marroquin, A., Schepanski, K., Semenkov, I., Sharapova, A., Shevnina, E., Shi, Z., Sofiev, M., Thevenet, F., Thorsteinsson, T., Timofeev, M., Umo, N. S., Uppstu, A., Urupina, D., Varga, G., Werner, T., Arnalds, O., and Vukovic Vimic, A.: Newly identified climatically and environmentally significant high-latitude dust sources, Atmospheric Chemistry and Physics, 22, 11 889–11 930, https://doi.org/10.5194/acp-22-11889-2022, 2022.

Meinander, O., Uppstu, A., Dagsson-Waldhauserova, P., Groot Zwaaftink, C., Juncher Jørgensen, C., Baklanov, A., Kristensson, A., Massling, A., and Sofiev, M.: Dust in the Arctic: a brief review of feedbacks and interactions between climate change, aeolian dust and ecosystems, Frontiers in Environmental Science, Volume 13 - 2025, https://doi.org/10.3389/fenvs.2025.1536395, 2025.

Mioche, G., Jourdan, O., Ceccaldi, M., and Delanoë, J.: Variability of mixed-phase clouds in the Arctic with a focus on the Svalbard region: a study based on spaceborne active remote sensing, Atmospheric Chemistry and Physics, 15, 2445–2461, https://doi.org/10.5194/acp-15-2445-2015, 2015.

Nakanishi, M. and Niino, H.: Development of an Improved Turbulence Closure Model for the Atmospheric Boundary Layer, Journal of the Meteorological Society of Japan. Ser. II, 87, 895–912, https://doi.org/10.2151/jmsj.87.895, 2009.

Niemand, M., Möhler, O., Vogel, B., Vogel, H., Hoose, C., Connolly, P., Klein, H., Bingemer, H., DeMott, P., Skrotzki, J., and Leisner, T.: A Particle-Surface-Area-Based Parameterization of Immersion Freezing on Desert Dust Particles, Journal of the Atmospheric Sciences, 69, 3077 – 3092, https://doi.org/10.1175/JAS-D-11-0249.1, 2012.

NOAA National Centers for Environmental Information: ETOPO 2022 60 Arc-Second Global Relief Model [Dataset], http://doi.org/10.25921/fd45-gt74, accessed 9-June-2026, 2022.

Okin, G. S., Mahowald, N., Chadwick, O. A., and Artaxo, P.: Impact of desert dust on the biogeochemistry of phosphorus in terrestrial ecosystems, Global Biogeochemical Cycles, 18, https://doi.org/https://doi.org/10.1029/2003GB002145, 2004.

Pino-Carmona, M., Ruiz-Arias, J. A., Fernández-Carvelo, S., Bravo-Aranda, J. A., and Alados-Arboledas, L.: Intercomparison of WRF-chem aerosol schemes during a dry Saharan dust outbreak in Southern Iberian Peninsula, Atmospheric Environment, 339, 120 872, https://doi.org/https://doi.org/10.1016/j.atmosenv.2024.120872, 2024.

Prospero, J. M.: Long-term measurements of the transport of African mineral dust to the southeastern United States: Implications for regional air quality, Journal of Geophysical Research: Atmospheres, 104, 15 917–15 927, https://doi.org/https://doi.org/10.1029/1999JD900072, 1999.

Raif, E. N., Barr, S. L., Tarn, M. D., McQuaid, J. B., Daily, M. I., Abel, S. J., Barrett, P. A., Bower, K. N., Field, P. R., Carslaw, K. S., and Murray, B. J.: High ice-nucleating particle concentrations associated with Arctic haze in springtime cold-air outbreaks, Atmospheric Chemistry and Physics, 24, 14 045–14 072, https://doi.org/10.5194/acp-24-14045-2024, 2024.

https://doi.org/10.5194/egusphere-2026-4112
Preprint. Discussion started: 21 July 2026

Raut, J.-C., Marelle, L., Fast, J. D., Thomas, J. L., Weinzierl, B., Law, K. S., Berg, L. K., Roiger, A., Easter, R. C., Heimerl, K., Onishi, T., Delanoë, J., and Schlager, H.: Cross-polar transport and scavenging of Siberian aerosols containing black carbon during the 2012 ACCESS summer campaign, Atmospheric Chemistry and Physics, 17, 10 969–10 995, https://doi.org/https://doi.org/10.5194/acp-17-10969-2017, 2017.

Raut, J.-C., Law, K. S., Onishi, T., Daskalakis, N., and Marelle, L.: Impact of shipping emissions on air pollution and pollutant deposition over the Barents Sea, Environmental Pollution, 298, 118 832, https://doi.org/https://doi.org/10.1016/j.envpol.2022.118832, 2022.

Sand, M., Samset, B. H., Balkanski, Y., Bauer, S., Bellouin, N., Berntsen, T. K., Bian, H., Chin, M., Diehl, T., Easter, R., Ghan, S. J., Iversen, T., Kirkevåg, A., Lamarque, J.-F., Lin, G., Liu, X., Luo, G., Myhre, G., Noije, T. V., Penner, J. E., Schulz, M., Seland, Ø., Skeie, R. B., Stier, P., Takemura, T., Tsigaridis, K., Yu, F., Zhang, K., and Zhang, H.: Aerosols at the poles: an AeroCom Phase II multi-model evaluation, Atmospheric Chemistry and Physics, 17, 12 197–12 218, https://doi.org/10.5194/acp-17-12197-2017, 2017.

Shao, Y., Ishizuka, M., Mikami, M., and Leys, J. F.: Parameterization of size-resolved dust emission and validation with measurements, Journal of Geophysical Research: Atmospheres, 116, https://doi.org/https://doi.org/10.1029/2010JD014527, 2011.

Shi, Y., Liu, X., Wu, C., Lu, Z., Zhang, K., and Ma, P.-L.: Representing Anthropogenic Dust From Agricultural Sources in E3SMv1: Implementation, Evaluation, and Assessment of the Radiative Forcing, Journal of Advances in Modeling Earth Systems, 17, e2023MS003 925, https://doi.org/https://doi.org/10.1029/2023MS003925, e2023MS003925 2023MS003925, 2025.

Skamarock, W., Klemp, J., Dudhia, J., Gill, D., Liu, Z., Berner, J., Wang, W., Powers, J., Duda, M., Barker, D., and Huang, X.-Y.: A Description of the Advanced Research WRF Model Version 4, Tech. rep., NCAR, https://doi.org/https://doi.org/10.5065/1dfh-6p97, 2019.

Sofiev, M., Vira, J., Kouznetsov, R., Prank, M., Soares, J., and Genikhovich, E.: Construction of the SILAM Eulerian atmospheric dispersion model based on the advection algorithm of Michael Galperin, Geoscientific Model Development, 8, 3497–3522, https://doi.org/10.5194/gmd-8-3497-2015, 2015.

Tewari, M., Chen, F., Wang, W., Dudhia, J., LeMone, M. A., Gayno, G., Wegiel, J., and Cuenca, R. H.: Implementation and verification of the unified Noah land surface model in the WRF model, in: 20th Conference on Weather Analysis and Forecasting/16th Conference on Numerical Weather Prediction, pp. 11–15, 2004.

Thomas, J. L., Polashenski, C. M., Soja, A. J., Marelle, L., Casey, K. A., Choi, H. D., Raut, J.-C., Wiedinmyer, C., Emmons, L. K., Fast, J. D., Pelon, J., Law, K. S., Flanner, M. G., and Dibb, J. E.: Quantifying black carbon deposition over the Greenland ice sheet from forest fires in Canada, Geophysical Research Letters, 44, 7965–7974, https://doi.org/https://doi.org/10.1002/2017GL073701, 2017.

Thompson, G. and Eidhammer, T.: A Study of Aerosol Impacts on Clouds and Precipitation Development in a Large Winter Cyclone, Journal of the Atmospheric Sciences, 71, 3636 – 3658, https://doi.org/10.1175/JAS-D-13-0305.1, 2014.

Thompson, G., Field, P. R., Rasmussen, R. M., and Hall, W. D.: Explicit Forecasts of Winter Precipitation Using an Improved Bulk Microphysics Scheme. Part II: Implementation of a New Snow Parameterization, Monthly Weather Review, 136, 5095–5115, https://doi.org/10.1175/2008MWR2387.1, 2008.

Tilmes, S., Emmons, L. K., Buchholz, R. R., and The CESM2 Development Team: CESM2.2 CAM-chem as Boundary Conditions, https://doi.org/10.5065/XS0R-QE86, 2022.

Tuccella, P., Thomas, J. L., Law, K. S., Raut, J.-C., Marelle, L., Roiger, A., Weinzierl, B., Denier van der Gon, H. A. C., Schlager, H., and Onishi, T.: Air pollution impacts due to petroleum extraction in the Norwegian Sea during the ACCESS aircraft campaign, Elementa: Science of the Anthropocene, 5, 25, https://doi.org/http://doi.org/10.1525/elementa.124, 2017.

Ukhov, A., Ahmadov, R., Grell, G., and Stenchikov, G.: Improving dust simulations in WRF-Chem v4.1.3 coupled with the GOCART aerosol module, Geoscientific Model Development, 14, 473–493, https://doi.org/10.5194/gmd-14-473-2021, 2021.

https://doi.org/10.5194/egusphere-2026-4112
Preprint. Discussion started: 21 July 2026

Ullrich, R., Hoose, C., Möhler, O., Niemand, M., Wagner, R., Höhler, K., Hiranuma, N., Saathoff, H., and Leisner, T.: A New Ice Nucleation Active Site Parameterization for Desert Dust and Soot, Journal of the Atmospheric Sciences, 74, 699 – 717, https://doi.org/10.1175/JAS-D-16-0074.1, 2017.

UNCCD: Sand and Dust Storms Compendium: Information and Guidance on Assessing and Addressing the Risks, Tech. rep., United Nations Convention to Combat Desertification, Bonn, Germany, 2022.

Whaley, C. H., Mahmood, R., von Salzen, K., Winter, B., Eckhardt, S., Arnold, S., Beagley, S., Becagli, S., Chien, R.-Y., Christensen, J., Damani, S. M., Dong, X., Eleftheriadis, K., Evangeliou, N., Faluvegi, G., Flanner, M., Fu, J. S., Gauss, M., Giardi, F., Gong, W., Hjorth, J. L., Huang, L., Im, U., Kanaya, Y., Krishnan, S., Klimont, Z., Kühn, T., Langner, J., Law, K. S., Marelle, L., Massling, A., Olivié, D., Onishi, T., Oshima, N., Peng, Y., Plummer, D. A., Popovicheva, O., Pozzoli, L., Raut, J.-C., Sand, M., Saunders, L. N., Schmale, J., Sharma, S., Skeie, R. B., Skov, H., Taketani, F., Thomas, M. A., Traversi, R., Tsigaridis, K., Tsyro, S., Turnock, S., Vitale, V., Walker, K. A., Wang, M., Watson-Parris, D., and Weiss-Gibbons, T.: Model evaluation of short-lived climate forcers for the Arctic Monitoring and Assessment Programme: a multi-species, multi-model study, Atmospheric Chemistry and Physics, 22, 5775–5828, https://doi.org/https://doi.org/10.5194/acp-22-5775-2022, 2022.

Wiedinmyer, C., Kimura, Y., McDonald-Buller, E. C., Emmons, L. K., Buchholz, R. R., Tang, W., Seto, K., Joseph, M. B., Barsanti, K. C., Carlton, A. G., and Yokelson, R.: The Fire Inventory from NCAR version 2.5: an updated global fire emissions model for climate and chemistry applications, Geoscientific Model Development, 16, 3873–3891, https://doi.org/10.5194/gmd-16-3873-2023, 2023.

Xu, K.-M. and Randall, D. A.: A Semiempirical Cloudiness Parameterization for Use in Climate Models, Journal of Atmospheric Sciences, 53, 3084 – 3102, https://doi.org/10.1175/1520-0469(1996)053<3084:ASCPFU>2.0.CO;2, 1996.

Zaveri, R. A., Easter, R. C., Fast, J. D., and Peters, L. K.: Model for Simulating Aerosol Interactions and Chemistry (MOSAIC), Journal of Geophysical Research: Atmospheres, 113, https://doi.org/10.1029/2007JD008782, 2008.

Zhao, A., Ryder, C. L., and Wilcox, L. J.: How well do the CMIP6 models simulate dust aerosols?, Atmospheric Chemistry and Physics, 22, 2095–2119, https://doi.org/10.5194/acp-22-2095-2022, 2022.